9

The Ion Cyclotron Resonance Hypothesis

A.R. Liboff

CONTENTS

9.1 Introduction

9.1.1 General Remarks

Ion cyclotron resonance (ICR) is one among a number of possible mechanisms that have been advanced to explain observed interactions between weak low-frequency electromagnetic fields and biological systems. Despite the failure to find a reasonable physical explanation, there remains an impressive body of experimental evidence that can be taken as an empirical basis for this hypothesis. The ICR suggestion has proven fruitful in framing both experimental and theoretical work, despite the biophysical situation being far from the literal cyclotron resonance model of an isolated classical charged particle moving in a vacuum under the influence of a magnetic field.

The properties of the applied fields that are used in ICR experiments include linear or circular polarization, the presence of a finite magnetostatic field, frequencies ranging from a few to several hundred hertz, magnetic intensities ranging from about 1 μT to 1 mT, and,

most important, a directional constraint on the relative orientation of the time-varying electromagnetic field to the magnetostatic (DC) field. This orientation requires that time-varying magnetic fields be parallel to the DC field or, equivalently, that time-varying electric fields are perpendicular to the DC field.

The ICR hypothesis holds that the physiological activity of those ions implicated in cell signaling processes, including, among others, Ca^{2+}, Mg^{2+}, and K^{+}, can be altered when the ratio of applied signal frequency to the static magnetic field is equal to the ionic charge-to-mass ratio. This is expressed as

$$\omega/B = q/m \tag{9.1}$$

where the radial frequency $\omega = 2\pi f$, as measured in radians per second, is used instead of f, the frequency measured in hertz. In SI units, B is the DC field intensity measured in tesla, and q/m is the ratio of the ionic charge to mass, in coulombs per kilogram. For any given ionic species, the specific frequency that equals the product of B and q/m is called the cyclotronic frequency, ω_c.

The resonance concept is attractive for a number of reasons. There is a potential connection to interactions involving the Earth's magnetic field (geomagnetic field [GMF]). Further, the ICR mechanism may help provide the basis for at least some of the reports of low-frequency electromagnetic interactions that otherwise lack explanation. Finally, given the wide variety of biological systems in which ICR effects are observed, it is reasonable to ask if there are fundamental scientific questions connected to this phenomenon.

The ICR hypothesis has especial significance attached to magnetostatic fields whose intensity is of the order of the GMF (20–60 μT). This becomes apparent when the charge-to-mass ratios of key biological ions are substituted into Equation 9.1. These ratios range from about 2 to 8×10^6 C/kg, implying that a static magnetic field of 50 μT corresponds to resonance frequencies of the order of 10–100 Hz (Figure 9.1). Such frequencies could

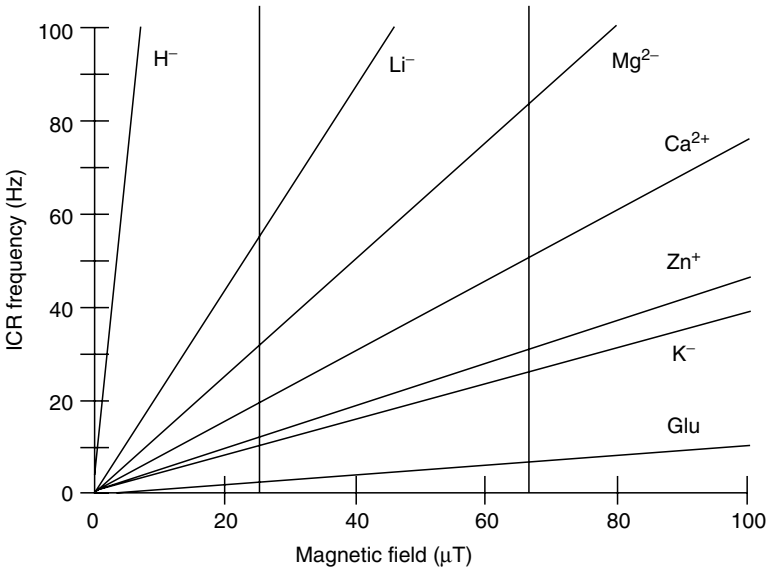

FIGURE 9.1
Ion cyclotron resonance frequencies for many biologically important ions in the Earth's magnetic field are in the ELF range.

TABLE 9.1

ICR Cation Possibilities

Ion	q/m (C/kg) $\times 10^{-6}$	f/B (Hz/μT)
H^+	95.76	15.241
Li^+	13.90	2.212
Mg^{2+}	7.937	1.263
H_3O^+	5.066	0.807
Ca^{2+}	4.814	0.766
Zn^{2+}	2.951	0.470
K^+	2.467	0.393
Arg^{2+}	1.235	0.197
Asn^+	0.838	0.133
Glu^+	0.747	0.119
Tyr^+	0.591	0.094

conceivably have physiological significance since they correspond approximately to the frequency range generated in the central nervous system [1]. This, coupled to the focus on the potential hazards attached to 50/60-Hz electromagnetic power delivery sources [2], has sparked study of the ICR hypothesis, in terms of both experiments specifically designed to test this hypothesis as well as theoretical models seeking an explanatory basis at the molecular level.

Some specific ions that have been implicated are listed in Table 9.1. Note that four polar amino acids and the hydronium ion are included. The ratios of frequency to DC magnetic field, as calculated from Equation 9.1, are shown in the right-hand column. This ratio can be regarded as an invariant characteristic for any given ion.

Although experimental evidence provides support for the ICR hypothesis [3], there is no widely accepted theoretical explanation. Indeed, because of constraints mainly arising from unfavorable damping conditions, there are strong arguments [4] against the occurrence in living tissue of any classical ICR mechanism [5], as occurs, say, for energetic charged particles moving in a vacuum under the influence of parallel static and AC magnetic fields. The circular and helical paths associated with such undamped motion are invariably the result of the Lorentz force, which imparts an acceleration **a** to a charged particle of mass m moving at velocity **v** in a magnetic field **B**:

$$\mathbf{a} = (q/m)(\mathbf{v} \times \mathbf{B}) \tag{9.2}$$

Nevertheless, arguments have been raised [6–11] that although the biological response may not correspond to the effects resulting from ICR-specific helical pathways of charged particles [4], the coupling is nevertheless a function of the ICR frequency as predicted by Equation 9.1. Although there has been no consistent experimental verification for any of these models, there is little question concerning the observed dependence on the cyclotron resonance frequency. Because the cyclotronic frequency is the common denominator in all these models, it is preferable to subsume all of them under the umbrella term ICR hypothesis.

The great variety of biosystems in which ICR effects have been observed implies a ubiquitous response that may have fundamental physiological significance. One can generalize this response R in terms of its functional dependence. From Equation 9.1, we can write

$$R = R(\omega, B, q/m) \tag{9.3}$$

Lednev [7] added a fourth variable, namely the intensity of the AC magnetic field, B_{AC}. Thus, the expanded expression for the response $R = R(\omega, B, B_{AC}, q/m)$, or, in terms of the two key variables,

$$R = R(\omega_c, B_{AC}) \tag{9.4}$$

There is no question as to the relevance of B_{AC} in studying the interactions between ICR field combinations and biological systems. However, it is not clear if the experimentally observed dependences on B_{AC} are a direct result of the underlying resonance mechanism, as has been suggested [7,9], or if there are other separate physiological factors that limit the levels of the AC field under which an ICR mechanism may be operative.

9.1.2 Background History

ICR was originally invoked [4] to explain an extraordinary set of observations by Blackman's group [12] indicating a strong dependence on the orientation of the magnetostatic field when studying the Ca-efflux model system [13]. The original discovery of the Ca-efflux effect [13] and subsequent studies [14–17] showed conclusively that the level of $_{45}Ca^{2+}$ efflux from preloaded chick brain was a nonlinear function of low-frequency (ca. 15 Hz) modulation signals when these brains were exposed to high-frequency carrier electric fields. Typically, this nonlinear signature (Figure 9.2), at first referred to as a ''window,'' has the appearance of a resonance curve. The Blackman experiment [12] discovered that this resonance signature appeared only when certain specific values of the vertical DC magnetic field were superposed on the system. In Table 9.2, ''Yes'' indicates the appearance of a resonance signature for a given combination of f and B.

In addition to Blackman's original set of results, a fourth column has been added in Table 9.2 to show the putative charge-to-mass ratio as determined from Equation 9.1. One sees that the sign of the magnetic field direction, either pointing up or down, does not affect the outcome. The specific combination of 15 Hz and 38 μT is positive, as is the combination of 30 Hz and 76 μT, suggesting that the ratio of frequency to field is involved as a key factor.

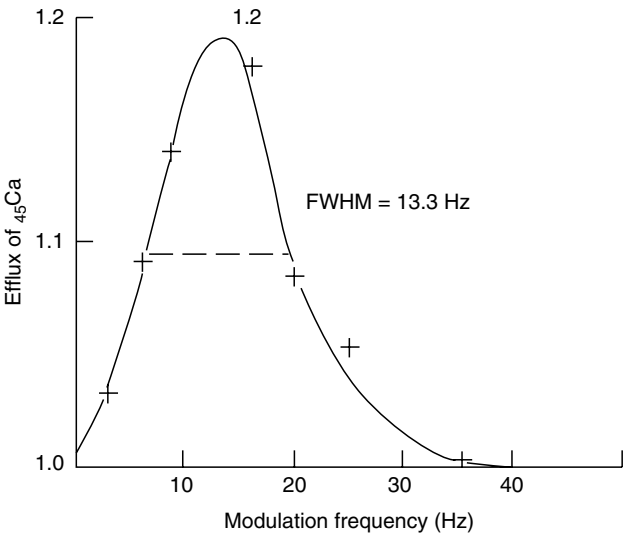

FIGURE 9.2
Comparison of shape of ''window'' data for Ca-efflux results [13] (seven points) with predicted resonance curve [18] (smooth curve). The best fit is for the charge-to-mass ratio for K^+, a magnetostatic field of 35.0 μT, and a collision time of 0.026 sec.

TABLE 9.2

Analysis of Blackman [12] Data

f (Hz)	B (μT)	Outcome	q/m (C/kg)
15	38	Yes	2.48×10^6
15	19	No	4.96×10^6
30	38	No	4.96×10^6
30	76	Yes	2.48×10^6
30	−76	Yes	2.48×10^6
30	50	No	3.77×10^6
30	25	Yes	7.54×10^6
30	−25	Yes	7.54×10^6
30	−83	No	2.27×10^6

Despite the fact that calcium was explicitly measured in this and the earlier Ca-efflux experiments, the data in Table 9.2 give reason to believe that the potassium ion was the primary target for the electromagnetic interactions. First, note that the charge-to-mass ratio of 2.48×10^6 C/kg is associated with positive outcomes. This ratio is less than 0.5% different from the q/m ratio for the potassium ion as shown in Table 9.1. The evidence linking K^+ to a positive outcome is further strengthened by examining the results obtained for the combination of 30 Hz and 25 μT. The positive outcome in this case suggests a q/m value of 7.54×10^6 C/kg, three times larger than the q/m ratio for K^+. In cyclotron resonance, one typically observes a set of resonance frequencies ω_n, where the fundamental at $n = 1$ is given in Equation 9.1, and the higher harmonic frequencies are restricted to the odd [19–21] harmonics $n = 3, 5, 7, \ldots$. The f/B ratio of 30/25 Hz/μT is nearly three times larger than the ratio 15/38 Hz/μT, again implying that the K^+ ion is interacting with the magnetic field, this time as a result of an excitation at the third harmonic.

There is further evidence that the K^+ ion is an important interactive factor in the nonlinear effects observed in the Ca-efflux experiments. McLeod and Liboff [18,22] derived the resonance signature for a charged particle as a function of frequency, showing that the relative conductivity, with and without the presence of an ion resonance field combination, is

$$\frac{\sigma_x}{\sigma_0} = \frac{(1 + (\omega_c + \omega)^2 \tau^2)}{\left(1 + [(\omega_c^2 - \omega^2)\tau^2]^2 + 4\omega^2\tau^2\right)} \tag{9.5}$$

This is a typical resonance expression that includes the effects of damping, expressed in terms of the collision time τ. By varying the choices of q/m ratios and collision times this expression can be directly compared to the results of Bawin and Adey [13], as shown in Figure 9.2. The smooth curve that best fits Equation 9.5 to the experimental points is also shown in Figure 9.2. This fitting procedure reveals that the most likely explanation for the data involves charged particles in cyclotron resonance with a q/m ratio equal to that of the potassium ion.

Thus, two independent sets of Ca-efflux data, one with DC magnetic fields applied as part of the experiment [12] and the other with the ambient magnetic field in the laboratory playing an unsuspected role [14], yield the same conclusion, that ICR stimulation of the K^+ ion results in the nonlinear resonance response.

9.2 Experimental Evidence

There is a surprisingly wide variety of biological systems in which ICR effects are observed. This suggests a heretofore unknown electromagnetic biological interaction. The model systems that have been examined in the literature can be conveniently divided into the categories of bone, cell culture, rat behavior, neural cell culture, diatom motility, complex biological systems, plants, and cell-free systems. These eight separate broad categories are listed respectively in Table 9.3 through Table 9.10. There is some

TABLE 9.3

ICR Effects in Skeletal Tissues

Frequency (Hz)	B_0 (μT)	Tuning	Ratio B/B_0	Comments	Reference
100	130	Ca^{2+}	1.0	Enhanced cell (fibroblast) proliferation; B varied between 50 and 500 μT	23
75	98	Ca^{2+}	1.0	Enhanced proliferation	23
16	42	Ca^{2+}	1.0	Enhanced proliferation	23
16	20.9	Ca^{2+}	1.0	Increases in rudiment length and midshaft diameter in embryonic chick femur	24
16	12.7	Mg^{2+}	1.0	Similar results to Ca^{2+} tuning	24
16	40.9	K^{+}	1.0	Results opposite to Ca^{2+} and Mg^{2+} cases: bone growth inhibited	24
80	20	Ca^{2+}/Mg^{2+}	1.0	Both fifth Ca^{2+} to third Mg^{2+} harmonics; enhanced collar thickness and length	24
72.6–80.6	20	Ca^{2+}	1.0	Resonance in IGF-II concentration at 76.6 Hz in osteosarcoma cell line	25
76.6	20	Ca^{2+}	1.0	Fifth harmonic: enhanced proliferation in osteosarcoma and human bone cells	25
15.3	20	Ca^{2+}	1.0	Reduction in tissue growth factor (TGF) β-1 inhibition in chondrocyte culture	26
25.4	20	Mg^{2+}	1.0	Reduction of TGF β-1 inhibition in chondrocyte culture	26
76.6	20	Ca^{2+}/Mg^{2+}	1.0	Reduction of TGF β-1 inhibition in chondrocyte culture	26
15.3	20	Ca^{2+}	1.0	Enhanced protoglycans synthesis in bovine cartilage	26
76.6	20	Ca^{2+}/Mg^{2+}	1.0	Mixed third and fifth harmonics reduce bone loss related to castration in rats	27
14.3–18.3	20		1.0	Increase in $_{45}Ca$ maximized at 16.3 Hz in osteosarcoma cell line	28
14.3–18.3	20		1.0	Increase in $_{45}Ca$ maximized at 15.3 Hz in a different osteosarcoma cell line	28
15.3	20	Ca^{2+}	1.0	370% increase in stiffness in ostectomized rabbit fibula after 24 h/28 d exposure	29
25.4	20	Mg^{2+}	1.0	137% increase in stiffness in ostectomized rabbit fibula after 24 h/28 d exposure	29
15.3	20	Ca^{2+}	1.0	Enhanced DNA synthesis and IGF-II levels in osteosarcoma cell line	30
13.3–17.3	20		1.0	Resonance maximum in IGF-II receptor number and affinity at 15.3 Hz	31
16	20.9	Ca^{2+}	1.0	Enhanced chick femoral diameter and glycosaminoglycans (GAGS) content	32
16	12.7	Mg^{2+}	1.0	Large (90%) GAGS enhancement	32
16	40.7	K^{+}	1.0	Opposite effects for Ca^{2+} and Mg^{2+} tuning, replicating Smith et al. [24]	32

TABLE 9.4

ICR Effects in Cell Culture

Frequency (Hz)	B_0 (μT)	Tuning	Ratio B/B_0	Comments	Reference
14.3	21	$_{45}Ca^{2+}$	1.0	Isotopic shift in q/m resonance confirmed, $_{40}Ca$ to $_{45}Ca$	33
14.3	21	$_{45}Ca^{2+}$	1.0	Threefold incorporation of $_{45}Ca$ into human lymphocytes	33
14.3	21	$_{45}Ca^{2+}$		Effect on human lymphocytes disappears at larger AC intensity	33
14.3	20.9	$_{45}Ca^{2+}$	1.0	2.3-fold uptake in $_{45}Ca$ disappears with addition of calcium blocker nifedipine	34
38.15	50	Ca^{2+}	1.0	No effect on Ca^{2+} in four different cell lines as observed using calcium fluorochrome fura-2	35
16	20.9	Ca^{2+}	1.0	Enhanced proliferation (46%) for fibroblast culture at Ca^{2+} ICR tuning	36
?	20.9	K^+	1.0	Reduced proliferation (18%) for Raji cells exposed to K^+ ICR; frequency not provided	36
13.6	16.5	$_{45}Ca^{2+}$	1.2	ICR frequency off by 3.5 Hz; enhanced $_{45}Ca^{2+}$ levels (75–126%) in three cell lines	37
60	20	$_{45}Ca^{2+}$	1.0	Fifth harmonic for $_{45}Ca^{2+}$ uptake is enhanced by 37%	37
16	23.4	$_{45}Ca^{2+}$	1.8	Decreased Ca^{2+} influx in mitogen-activated lymphocytes but no effect on resting cells	38
16	51.1	K^+	1.0	Third harmonic: enhanced proliferation of lymphoma cells; very narrow FWHM[a]	39
16	40.9	K^+	1.0	Enhanced proliferation of human lymphoma cells	39
16	23.4	Ca^{2+}	3.8, 5.3	No change in Ca^{2+} influx at AC/DC ratio of 3.8 but enhanced influx at ratio of 5.3	40
16	20.9	Ca^{2+}	1.4	No effect on mouse lymphocytes as observed using Ca fluorochrome Quin-2	41
50	65.3	Ca^{2+}	1.4	No effect on mouse lymphocytes with and without mitogenic stimulation	41
5–100	50–60	$?Ca^{2+}$	2.3–3.0	Enhanced calcium oscillations over broad frequency range, maximized at 50 Hz	42
32	42	Ca^{2+}	2.5, 5.0	Increased micronuclei formation in human lymphocytes at Ca^{2+} ICR tuning	43
32.50	0			No change in micronuclei formation when DC field is zero	43
15.3	20	Ca^{2+}	1.0	ICR effect on fura-2 calcium activity only found for added serum in cell medium	44
76.6	20	Ca^{2+}	1.0	Fifth harmonic is also successful	44
100	130	Ca^{2+}	1.9	Another ICR fundamental successful	44
100	130	Ca^{2+}	2.8	Repeating ICR application to primary bone cell culture at higher AC intensity	44

[a]FWHM, full width at half maximum.

unavoidable overlap among these, particularly in Table 9.3 (skeletal systems), where references to bone research in cell cultures and animals are grouped together.

Although most of the reports summarized in Table 9.3 through Table 9.10 lend considerable weight to the hypothesis that ICR magnetic stimulation can affect biological systems, the effects on diatom motility (Table 9.7) are not as clear-cut, in that a number of observers [62–65] failed to find any effects whatsoever. The explanation for the poor reproducibility in this case may rest with difficulties in handling the diatom model system, one that is especially sensitive to sample preparation.

TABLE 9.5

ICR Effects on Rat Behavior

Frequency (Hz)	B_0 (μT)	Tuning	Ratio B/B_0	Comments	Reference
60	26	Ca^{2+}	1.9	Third harmonic: loss of short-term (temporal) memory in rats	45
60	26	Ca^{2+}	1.9	Third harmonic: AC threshold observed (27 μT) for above results	46
60	27	Ca^{2+}	1.9	Third harmonic: learning inhibited relative to controls	47
60	48	Mg^{2+}	1.0	Learning enhanced relative to controls	47
60	26	Ca^{2+}	1.9	Third harmonic: no effect	48
50	65	Ca^{2+}		Reduced short-term memory and aggressiveness	49
630	500	Mg^{2+}	0.5	Enhanced exploratory activity	50
380	500	Ca^{2+}	0.5	Reduced exploratory activity	50
63	50	Mg^{2+}	0.7	Enhanced locomotor and exploratory activity	51
38	50	Ca^{2+}	0.7	Reduced locomotor and exploratory activity	51
630	500	Mg^{2+}	0.7	Enhanced locomotor and exploratory activity	51
380	500	Ca^{2+}	0.7	Reduced locomotor and exploratory activity	51

TABLE 9.6

ICR Effects on Neural Cell Culture

Frequency (Hz)	B_0 (μT)	Tuning	Ratio B/B_0	Comments	Reference
16	15–40.8	? Co^{2+} or Fe^{2+}?	0.5–1.3	Enhanced proliferation over controls (60%) in neuroblastoma cell culture	52
16	15–40.8		0.5–1.3	Decreased neurite outgrowth for ?Co^{2+}/Fe^{2+} ICR stimulation; possible Na^{+} ICR effect?	52
15.3	20	Ca^{2+}	1.0	Ca^{2+} tuning increases rate of neuronal differentiation in PC-12 cells	53
45	36.6	Mg^{2+}	0.03–1.81	Changes in neurite outgrowth for Mg^{2+} ICR at different AC intensities in PC-12 cells	54
25	20.3	Mg^{2+}	0.54–1.26	Similar Mg^{2+} ICR effect on PC-12 neurite outgrowth at another frequency	54
45	2.96	H^{+}	0.14–2.0	H^{+} ICR alters PC-12 neurite outgrowth	55
30	1.97	H^{+}	0.57–1.4	Similar effects at different ICR combinations	55
45	59	Ca^{2+}	0.26–1.49	PC-12 cells at Ca^{2+} ICR exhibit changes in neurite outgrowth at different AC intensities	56
42.5–47.5	2.97	H^{+}	0.56–1.5	Bandwidth for PC-12 neurite outgrowth due to H^{+} ICR is ±10%	57
40, 50	2.97		0.56–1.5	No effect	57

TABLE 9.7

ICR Effects on Diatom Motility

Frequency (Hz)	B_0 (μT)	Tuning	Ratio B/B_0	Comments	Reference
5–32	20.9		1.0	Maximum motility occurs at 16 Hz when Ca^{2+} concentration is 0.25 nM; no effect when fields are at 90°	58
16	20.9	Ca^{2+}	0.0–3.0	Motility maximized when B/B_0 ratio is 1	58
16	20.9	Ca^{2+}	0.7	Enhanced motility	59
32	20.9	Ca^{2+}	0.7	Even harmonic: no effect	59
48	20.9	Ca^{2+}	0.7	Third harmonic: enhanced motility	59
64	20.9	Ca^{2+}	0.7	Even harmonic: no effect	59
8	10.45	Ca^{2+}	1.4	Enhanced motility	60
12–64	15.7–83.6	Ca^{2+}		Additional ICR frequencies at 12, 16, 23, 31, 32, 46, 64 Hz also enhance motility	60
24, 40, 120	10.45	Ca^{2+}	1.4	Three ICR harmonics for 10.45 μT (n = 3, 5, 15) enhance motility	60
16–136	10.45	Ca^{2+}	1.40.73	Thirteen other frequencies (n = 2, 4, 6, 7, 8, 9, 10, 11, 12, 13, 14, 16, 17) fail to show effect	60
8	20.45	K^+	0.73	Motility inhibited	60
16	41	K^+	0.37	Motility inhibited	60
24, 40, 120	20.45	K^+	0.37	Three ICR harmonic frequencies for B_0 = 20.45 μT (n = 3, 5, 15) also inhibit motility	60
16–136	20.45	K^+	0.37	Thirteen other frequencies (n = 2, 4, 6, 7, 8, 9, 10, 11, 12, 13, 14, 16, 17) fail to show effect	60
16	21	Ca^{2+}	1.0	Enhanced motility	61
16	20.9	Ca^{2+}	1.0	No effect on motility	62
30	39.2	Ca^{2+}	1.0	No effect on motility	62
60	78.4	Ca^{2+}	1.0	No effect on motility	62
16	20.9	Ca^{2+}	1.0	No effect on motility	63
16	21	Ca^{2+}	1.0	No effect on motility	64
16	20.9	Ca^{2+}	1.0	No effect on motility as viewed with real-time video system	65

9.2.1 Rat Behavior

On the other hand, some of the experimental evidence merits special emphasis because of the way the results have been positively replicated and reinforced. This is particularly true of the work on rat behavior (Table 9.5), in which four independent groups [45,47,49,51] observed significant changes in behavior for ICR exposures that were tuned to either the calcium or the magnesium ion. The end points of these experiments included changes in short-term memory [45,51], learning capacity [47], and aggressiveness [49], behavioral factors that are conceivably interconnected. Most important, these were undoubtedly resonance effects, since changes were not observed when separate runs were made for exposures to either the AC magnetic field alone or the DC magnetic field alone. Only when the AC and DC magnetic fields were jointly applied and parallel and, moreover, when the combined field characteristics conformed to Equation 9.1 were the altered behavioral responses observed.

An interesting possible explanation for the neural interaction site in these experiments has been proposed by Lovely et al. [47,92]. Using a Y-maze setup this group observed precisely opposite learning abilities for Ca^{2+} tuning and for Mg^{2+} tuning. Since the ICR combined field affects learning capacity oppositely for Ca^{2+} tuning and Mg^{2+} tuning, it may be reasonable to assume that the glutamate receptor *N*-methyl D-aspartate (NMDA) is

TABLE 9.8

ICR Effects on Complex Biological Systems

Frequency (Hz)	B_0 (μT)	Tuning	Ratio B/B_0	Comments	Reference
3–770	10–220		0064–2.8	No effect on turtle colon transepithelial current as measured in Ussing chamber	66
33.7	44	Ca^{2+}	1.41	Synthesis and release of rat pineal melatonin is reduced by Ca^{2+} ICR tuning	67
15	21	Ca^{2+}	6.7	Fluctuations in heart rate in Daphnia are maximized at Ca^{2+} ICR frequency	68
60	78.4	Ca^{2+}	0.13	Cephalic regeneration in planaria is delayed by 48 h	69
60	51.1	K^+	1.0	Regeneration rate unchanged when K^+ tuning is used instead of Ca^{2+} tuning	69
60	78.4	Ca^{2+}	0.51	Regeneration anomalies occur at Ca^{2+} tuning when larger AC intensity is used	70
16	20.9	Ca^{2+}	1.8	Enhanced rate of blastema growth during cephalic regeneration in planaria	71
16	20.9	Ca^{2+}	0.24–9.6	Evidence that ICR effect on planaria regeneration has an intensity window	71
30	39.1	Ca^{2+}	1.8	Evidence corroborating Lednev [7] prediction: ICR effects are maximized at AC/DC ratio of 1.8	72
60	78.1	Ca^{2+}	1.8	Effect of light on ICR modulation of snail opioid analgesia is independent of frequency	72
120	156.2	Ca^{2+}	3.6	Effect due to light appears to scale with DC intensity	72
60	78	Ca^{2+}	0–5.3	Ca^{2+} ICR variations with AC intensity support Lednev [7] model	73
30	76	K^+	0–2.8	K^+ ICR effects on snail opioid analgesia are reversed with K^+ channel blocker	73
35	45	Ca^{2+}	1.8	Maximum influence on bioluminescence of dinoflagellate, agreement with PRM model	74
35	45	Ca^{2+}	5.3	Influence reversed, again in agreement with PRM model	74
35	45	Ca^{2+}	3.8	No effect at ratio of 3.8, again in agreement with PRM model	74

involved. NMDA receptors act as a graded switch for memory formation, to enhance learning and memory [93], and it is well established that NMDA activity is differently sensitive to calcium and magnesium concentrations [94,95]. Similar reversals of behavioral outcome depending on which ions are tuned have been observed by Zhadin et al. [51].

This explanation also serves to reinforce the original suggestion [4] concerning the molecular explanation for ICR stimulation, namely, in terms of enhanced ionic permeability within ion channels. Further support for locating the ion channel as the site of magnetic interaction is the fact that the changes in Ca^{2+} concentration within the cell that result from ICR stimulation tuned to the Ca^{2+} ion are not observed with the addition of nifedipine [34], a well-known calcium ion channel blocker (Figure 9.3).

9.2.2 Plants

Highly consistent results have also been independently obtained in studying the effects of ICR stimulation on plant growth [75–77,96] and seed germination [20,78] (Table 9.9,

TABLE 9.9

ICR Effects on Plants

Frequency (Hz)	$B_0(\mu T)$	Tuning	Ratio B/B_0	Comments	Reference
60	78.3	Ca^{2+}	0.26	Ca^{2+} ICR field combination stimulates radish growth after delaying germination	75
60	153.3	K^+	0.13	K^+ ICR field enhances germination while reducing growth	75
60	0			No effect	75
60	78.4	Ca^{2+}	0.26	Ca^{2+} fundamental stimulates growth but slows down germination	20
60	39.2	Ca^{2+}	0.51	Ca^{2+} second harmonic: no effect	20
60	26.1	Ca^{2+}	0.77	Ca^{2+} third harmonic: same result as Ca^{2+} fundamental	20
60	153.3	K^+	0.13	K^+ fundamental results opposite to those of Ca^{2+}: growth inhibited, germination enhanced	20
60	76.6	K^+	0.26	K^+ second harmonic results weakly opposite to fundamental and third harmonics	20
60	51.1	K^+	0.39	K^+ third harmonic: effect same as K^+ fundamental	20
60	47.5	Mg^{2+}	0.42	Mg^{2+} fundamental stimulates growth	20
60	9.5	Mg^{2+}	2.11	Mg^{2+} fifth harmonic stimulates growth	20
60	0			AC only: no effect	20
60	78.3	Ca^{2+}	0.26	Replication of Smith et al.'s [75] work	76
60	78.3	Ca^{2+}	0.26	No effect on mustard plant; possible effect on barley plant	76
50	65.3	Ca^{2+}	0.61	Replication of Smith et al.'s [75] work on radish, for the 50-Hz Ca^{2+} ICR condition	77
50	39.6	Mg^{2+}	0.60	Replication of Smith et al. [75] for 50-Hz Mg^{2+} condition	77
60	76.3	Ca^{2+}	0.26	Germination weakly enhanced following Ca^{2+} ICR exposure of dry radish seeds	78
60	153.5	Mg^{2+}	0.13	No effect on germination	78
60	47.6	K^+	0.42	Significantly greater (earlier) germination of dry seeds following K^+ ICR exposure	78
35.8	46.5	Ca^{2+}	1.84	Gravitropic response in millet, flax, and clover seedlings enhanced by Ca^{2+} ICR	79
58.7	46.5	Mg^{2+}	1.84	Gravitropic response unaffected by Mg^{2+} tuning	79
54.7	46.5	K^+	1.84	Gravitropic response inhibited by K^+ ICR	79
33.8–37.8	46.5	Ca^{2+}	1.84	Frequency-dependent gravitropic response exhibits Ca^{2+} peak: FWHM[a] = 1.6 Hz	80
60	48	Mg^{2+}	1.48	CO_2 uptake significantly below control in radish, replication of Smith et al. [75]	81

[a]FWHM, full width at half maximum.

Figure 9.4). The approach in the earlier reports [75] involved direct observations of aspects of plants that are readily measurable: plant height, aboveground height, root mass, stem diameter, leaf length, and width. Remarkably, all aspects related to growth are significantly affected, suggesting that magnetic fields play some unknown role in plant physiology. As observed in other systems (see Table 9.3), Ca^{2+} and Mg^{2+} tuning tends to enhance growth while tuning to the potassium ion acts as an inhibitor. Radish (*Raphanus sativus*) was used because of its rapid growth cycle (21 d), ease of handling, and seed availability. Davies [76] observed positive results when stimulating radish with ICR

TABLE 9.10

ICR Effects in Cell-Free Systems

Frequency (Hz)	B_0 (μT)	Tuning	Ratio B/B_0	Comments	Reference
8–20	20.9		1.0	Three frequencies (13.0, 14.0, and 16.0) affect calmodulin-dependent phosphorylation	82
100	0–260		>0.45	No Ca^{2+} ICR effect on conductance in pure bilipid layer	83
50–120	0–299		>0.31	Binding of Ca^{2+} to calmodulin is not enhanced using Ca^{2+} ICR fields	84
20	50	K^+	1.4	No changes from ICR tuning in gram A channel conductance in lipid bilayer	85
760	50	H^+	15.2	No changes from ICR tuning in gram A channel conductance in lipid bilayer	85
0.1–40	25	Asn^+	0.002	Enhanced aqueous conductivity in asparagine solution at 2.9 Hz; ICR prediction 2.9 Hz	86
0.1–40	25	Arg^{2+}	0.002	Enhanced aqueous conductivity in arginine solution at 4.4 Hz; ICR prediction 4.4 Hz	86
0.1–40	25	Glu^+	0.002	Enhanced aqueous conductivity in glutamic acid solution at 2.5 Hz; ICR prediction 2.6 Hz	86
0.1–40	25	Tyr^+	0.002	Enhanced aqueous conductivity in glutamic acid solution at 1.9 Hz; ICR prediction 2.1 Hz	86
0.1–40	25		0.2	ICR effect disappears at higher ratio of AC to DC intensities	86
0.1–40	0		0.002	ICR effect disappears for very small DC fields	86
0.1–40	25		0.002	ICR effects disappear when AC magnetic field is at 90° to DC field	86
12–60	20.9		1.0	No change in Ca^{2+} transport through patch-clamped cell membrane	87
10–22	20.9		1.0	No change in Ca^{2+} transport through patch-clamped system, measured over loner times	87
1–10	20–40	Glu^+	625–1.25 (×.001)	Changes in glutamic acid conductivity in solution; good agreement with Glu^+ ICR q/m prediction	88
1–10	40		0.25–2.0 (×.001)	Confirmation of earlier work; amino acid response at AC levels of 0.02–0.04 μT	88
0–10	40	Arg^{2+}	0.001	Sharp change in conductivity observed at 7.1 Hz, the ICR tuning point for Arg^{2+}	11
20.6	48	$H_3O^+(H_2O)$	0.02	ICR fields trigger long-term increases in electrical conductivity in pure water	89
40.1	48	H_3O^+	0.02	Data in agreement with ICR effect in hydronium ion	89
530	35	H^+	0.03	Data in agreement with ICR effect in proton	89

TABLE 9.10 (continued)

ICR Effects in Cell-Free Systems

Frequency (Hz)	B_0 (μT)	Tuning	Ratio B/B_0	Comments	Reference
16	20.9	Ca^{2+}	1.0	Binding of Ca^{2+} to calmodulin is not enhanced using Ca^{2+} ICR fields	90
25.4	37	$_{45}Ca^{2+}$	0.70	$_{45}Ca^{2+}$ efflux in plasma membrane vesicles: ICR peak observed	91
24	37		0–3.2	Agreement with Blanchard and Blackman's [9] IPR model	91

magnetic fields but reported observing no similar effect in mustard plants, implying that the influence on growth may be species specific. ICR effects on radish metabolism were also reported by Yano et al. [81] using a distinctly different assay, the rate of uptake of CO_2 as a surrogate for photosynthesis activity. Still another assay [97] that responds to ICR magnetic stimulation in radish is the optical transmittivity in leaf.

The work in radish was extended [96] to four species of orchid (*Brassavola*, *Encyclium*, *Phalaenopsis*, and *Bulbophuyllum*) (Figure 9.4 and Figure 9.5), with the magnetic exposures tuned to Ca^{2+} ICR lasting months instead of days. In all treated cases, plant heights were significantly higher compared to controls.

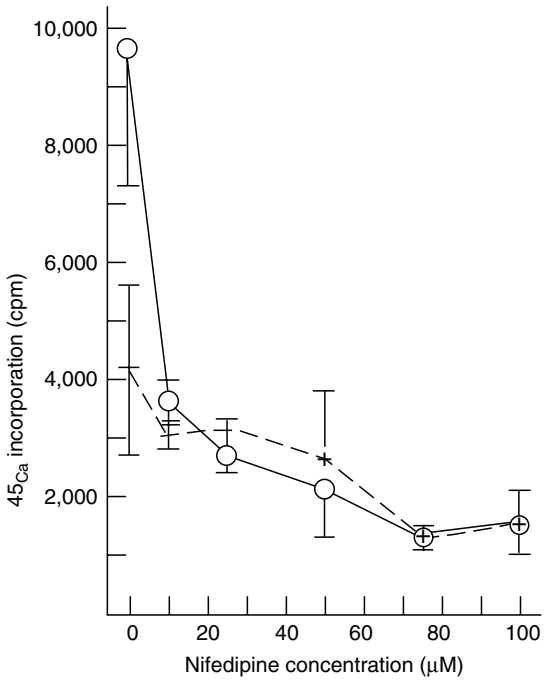

FIGURE 9.3

Incorporation of $_{45}Ca$ in human lymphocytes for unexposed cells (dashed line) and for ICR exposure tuned to the isotopic mass of $_{45}Ca$ (solid line) after 1 h. In the absence of calcium blocker nifedipine, there is a greater than twofold increase in calcium concentration over controls. The addition of nifedipine completely blocks the calcium uptake resulting from ICR stimulation, providing evidence that the ICR mechanism is related to ion channel transport. (From Rozek, R.J., Sherman, M.L., Liboff, A.R., McLeod, B.R., and Smith, S.D., Nifedipene is an antagonist to cyclotron resonance enhancement of $_{45}Ca$ incorporation in human lymphocytes, *Cell Calcium*, 8, 413, 1987.)

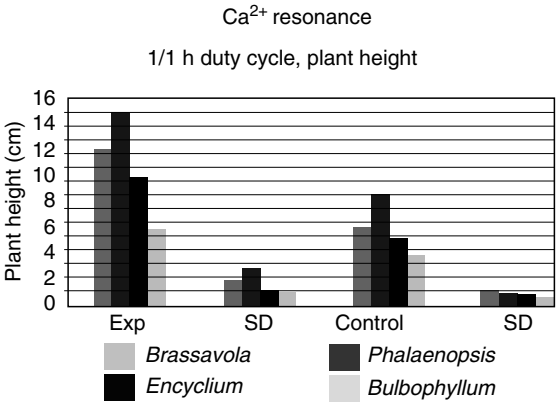

FIGURE 9.4
Comparisons of mean plant heights for four orchid varieties between unexposed controls and plants subjected to Ca^{2+} ICR stimulation. SD, standard deviation. (From Smith, S.D., Liboff, A.R., and McLeod, B.R., Calcium ICR and seedling growth in orchids (abstract), 20th Annual Meeting, Bioelectromagnetics Society, St. Petersburg Beach, FL, 1998.)

A distinctly different type of plant experiment has examined the rate of seed germination [21,78] instead of growth. In this case the assay simply involves a comparison of the time it takes for the seedling to be observed after the exposed seed is planted to the time it takes for a nonexposed seed to emerge. Unlike what is observed when examining growth rates, germination rates are significantly enhanced under K^+ stimulation and inhibited for Ca^{2+} tuning.

9.2.3 Bone

Elaborating on earlier work that used high-intensity pulsed magnetic fields [98] to treat bone disorders, ICR stimulation, operating at a much lower intensity, has proven very useful in repairing bone nonunions [29,99] and as an adjunct in enhancing spinal fusion following surgery [99]. Both these medical applications are approved by the U.S. Food and Drug Administration (FDA) and have been used to treat more than 100,000 patients in the United States [99]. There are two great advantages in these applications compared

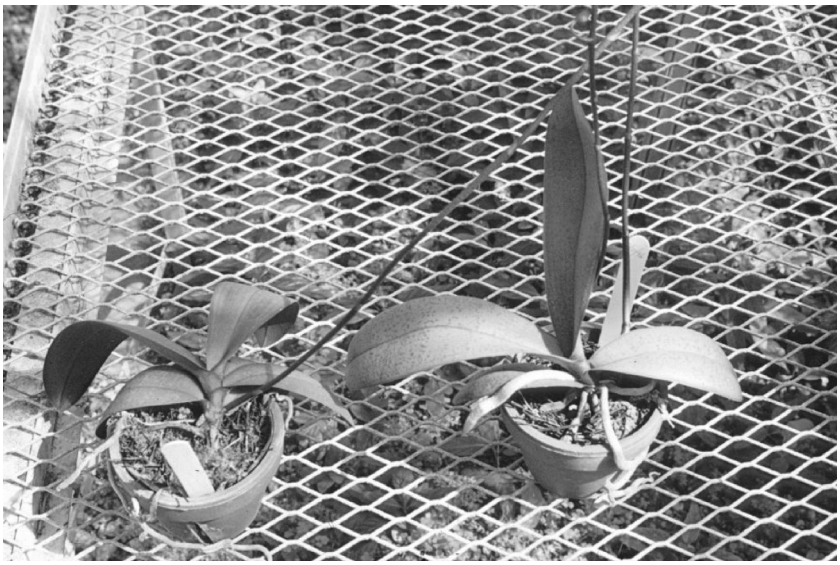

FIGURE 9.5
Typical example of difference between treated (right) and unexposed (left) orchid (*Phalaenopsis*) plants. (From Smith, S.D., Liboff, A.R., and McLeod, B.R., Calcium ICR and seedling growth in orchids (abstract), 20th Annual Meeting, Bioelectromagnetics Society, St. Petersburg Beach, FL, 1998.)

to pulsed magnetic fields therapy. Much weaker AC magnetic field intensities, less than 0.1 mT in amplitude, are employed, requiring very small power and providing the patient with greater portability. The treatment is also more efficient, requiring only 30 min/d during the therapeutic regimen.

This FDA-approved ICR device (Figure 9.6) also makes use of harmonic frequencies. The orientation of the local GMF relative to the plane of the AC coil is sensed, and the frequency of the applied sinusoidal magnetic signal generated by the coil is automatically adjusted to be in cyclotron resonance with the GMF following the relation $\omega_n = nqB/m$, where n is an integer representing either the third or the fifth ICR harmonic. Table 9.11 lists the ICR harmonics for a number of ions. In the case of bone, tuning to either Ca^{2+} or Mg^{2+} tends to stimulate bone growth [24] (Figure 9.7 and Figure 9.8). The FDA-approved device makes use of this fact by employing one resonance condition (3.80 Hz/μT) that fits both types of stimulation, namely the third harmonic for Mg^{2+} and the fifth for Ca^{2+}.

It is likely that the level of efficacy of ICR magnetic treatment in repairing bony nonunions is far from optimal. There is good evidence [9,73,82] that the ICR response may depend on the ratio of the AC to DC magnetic fields that are used in combination. As such, one can expect the search for improvements in therapeutic signals for bone repair to continue.

FIGURE 9.6
Device used to assist repair of bony nonunions. The two rectangular parallel coils are clamped over the defect, and the GMF component normal to the plane of these coils is automatically determined regardless of limb orientation. An AC magnetic field is applied parallel to the GMF field that is in ion resonance tuned to harmonics of calcium and magnesium. (Courtesy of OrthoLogic Corp., Tempe, AZ.)

TABLE 9.11

ICR Harmonics for Selected Ions

Ion	Fundamental (Hz/μT) f/B	Higher Harmonics (Hz/μT) $3f/B$	$5f/B$	Subharmonics (Hz/μT) $f/3B$	$f/5B$
Mg^{2+}	1.26	3.79	6.31	0.421	0.253
Ca^{2+}	0.77	2.30	3.83	0.255	0.153
Zn^{2+}	0.47	1.41	2.35	0.157	0.094
K^{+}	0.39	1.18	1.97	0.131	0.026

In attempting to further probe the response of skeletal tissues to resonant magnetic fields, Ryaby and colleagues [25–28,30,31] reported a number of associated metabolic changes in bone cells, most notably an increase in insulin-like growth factor-II (IGF-II) expression (Figure 9.9 and Figure 9.10) under ICR tuning for Ca^{2+}. This body of work was rather complete in that separate experiments were carried out to justify Equation 9.1. With the magnetostatic field held at one value the frequency was varied as shown in Figure 9.10. In addition, separate runs were made with a fixed frequency and different values of the DC magnetic field. Resonance peaks were observed for both arrangements in accordance with Equation 9.1.

9.2.4 Harmonics

In general, the question of which harmonics are observed in the experimental data remains unresolved. McLeod et al. [59], studying diatom motility, showed that when the DC field is kept constant, odd multiples of the ICR fundamental frequency also result in enhanced motility. The same type of frequency harmonic dependence was found for ICR stimulation of plant growth [21]. Similar experimental results were obtained by Blackman et al. [100] in determining the degree of radioactive calcium flux from chick

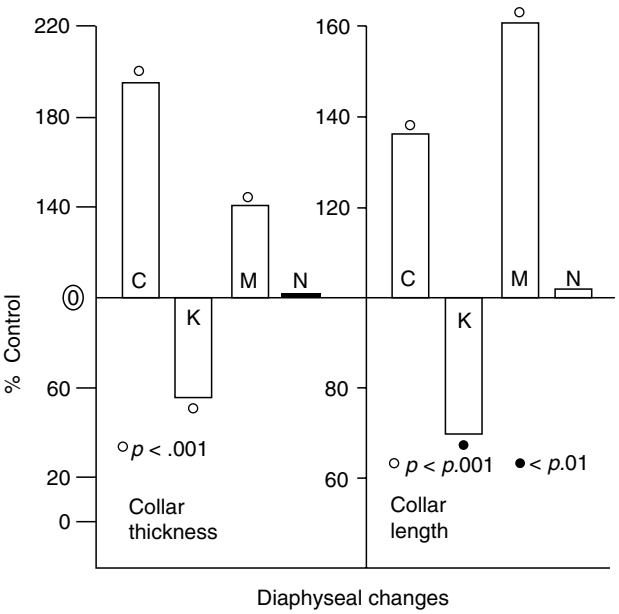

FIGURE 9.7
Ca^{2+} and Mg^{2+} ICR exposures aid bone growth. Changes in diaphysis of embryonic chick femur due to ICR stimulation are shown as percentage of controls. C and M correspond to Ca^{2+} and Mg^{2+} tuning, and K represents the effects of tuning to the q/m ratio for K^{+}. Note the reversal of effect following exposure to potassium-tuned magnetic fields. (From Smith, S.D., Liboff, A.R., and McLeod, B.R., Effects of resonant magnetic fields on chick femoral development *in vitro*, *J. Bioelectr.*, 10, 81, 1991.)

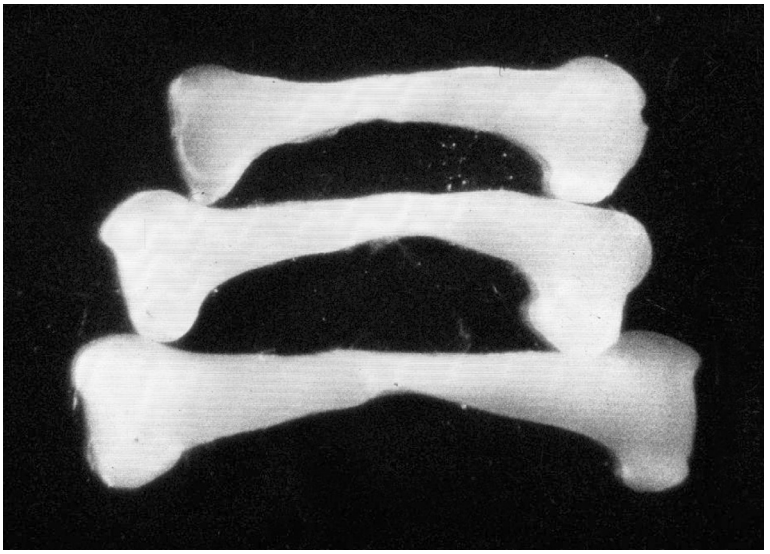

FIGURE 9.8
Typical examples of changes in embryonic chick femora with different ICR exposures. The longest femur corresponds to calcium ion stimulation, the shortest femur to potassium tuning, and the in-between size is the control. (From Smith, S.D., Liboff, A.R., and McLeod, B.R., Effects of resonant magnetic fields on chick femoral development *in vitro*, *J. Bioelectr*., 10, 81, 1991.)

brain as a function of electric-field modulation frequency. These various findings are in reasonable agreement with the predicted higher harmonic ICR signatures listed in Table 9.11.

Because subharmonics are predicted [7,101] in several theoretical models, the first two predicted odd subharmonic characteristics are also listed for convenience in Table 9.11. It

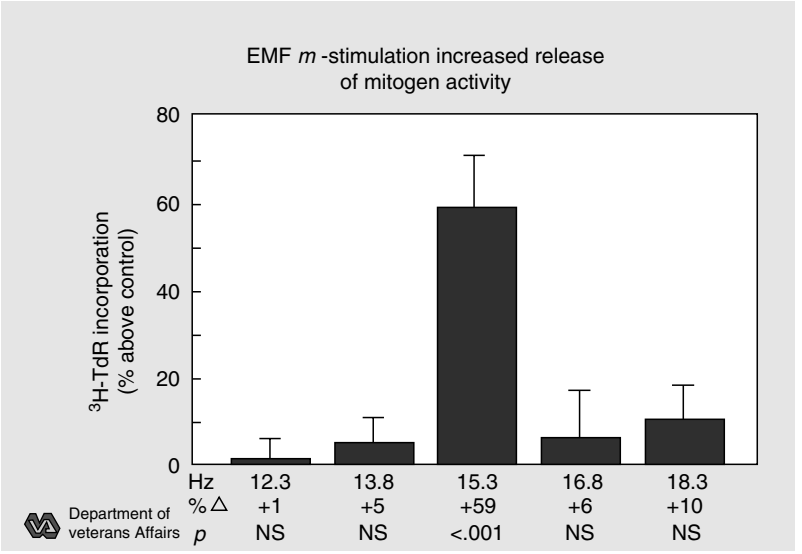

FIGURE 9.9
A sharp increase in mitogen expression in osteosarcoma cells exposed to a 20-μT DC magnetic field occurs when the AC magnetic field frequency is 15.3 Hz, corresponding to Ca^{2+} resonance. (Courtesy of Veterans Administration Hospital, Phoenix, AZ.)

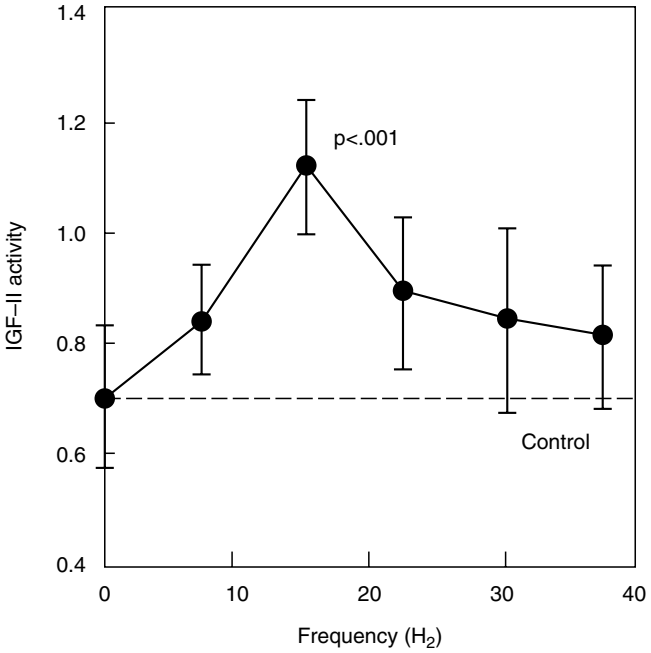

FIGURE 9.10
Peak in IGF-II expression at the fifth harmonic for Ca^{2+}. (Courtesy of J. Ryaby.) Fitzsimmons, R.J., Ryaby, J.T., Magee, F.P., and Baylink, D.J., Combined magnetic fields increase insulin-like growth factor-II in TE-85 human octeosarcoma bone cell cultures, *Endocrinology*, 136, 3100, 1995.)

is clear that a better fit between the theoretical predictions of harmonics and the nature of their experimental observations could be an important factor in further understanding of ICR phenomena in living things.

9.2.5 Physiological Reversals

There is substantial evidence [102] that changing the ICR tuning from one ionic species to another has the capacity to completely reverse physiological outcomes (Figure 9.8 and Figure 9.11). This has been reported in a number of separate fascinating observations in widely different ICR experiments. The effect is manifested by applying, at the same frequency, relatively small shifts in the local magnetic field or, equivalently, applying a changed frequency with the local magnetic field kept the same, both variations made according to Equation 9.1. Eight such sets of results are given in Table 9.12.

This type of opposite response in the data may provide an important clue in trying to understand the ICR effect at the molecular level. Such a response might be expected when looking at the effects of competitive ion concentrations on cell metabolism and signaling. One such example, mentioned above [47], is the difference in the effects of binding Ca^{2+} and Mg^{2+} to NMDA. The concentration of Ca^{2+} in the cytoplasm, itself an implicit function of other ionic concentrations, is carefully regulated through the use of calcium pumps. The production of key enzymes such as cyclic AMP is enhanced or inhibited depending on the cytoplasmic calcium ion concentration. Because of this it is reasonable to think that the action of ICR fields has its origin in membrane-bound ion channels or in those proteins involved in the cell-signaling process.

9.2.6 Water

There have been numerous puzzling reports [103–105] claiming that the physical properties of water (e.g., conductivity) can be sufficiently altered by exposure to magnetic

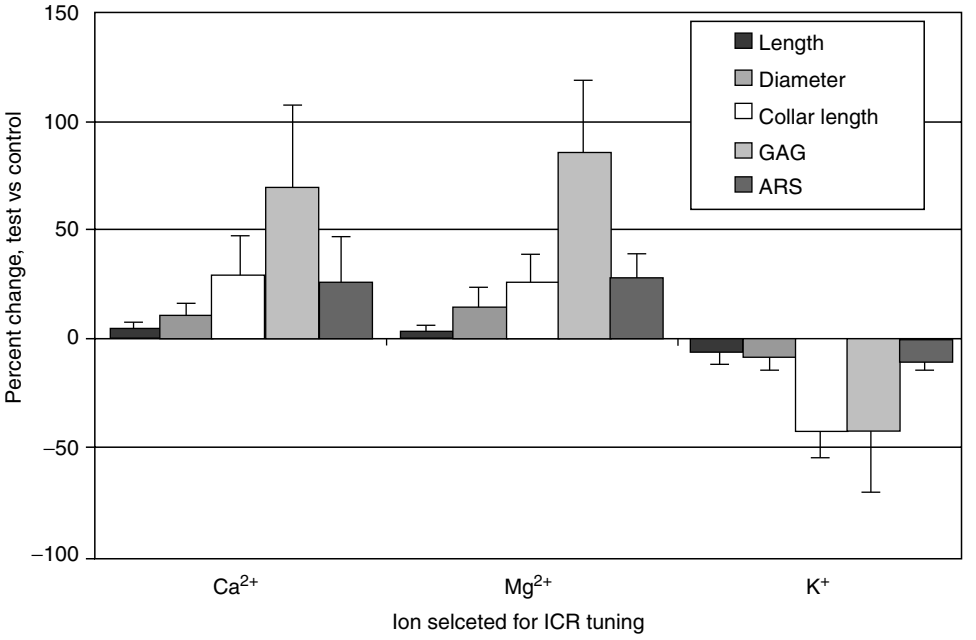

FIGURE 9.11
Independent confirmation of the results shown in Figure 9.8 for embryonic chick femur [32]. The additional assay for glycosaminoglycans (GAGS) reveals a greatly increased production of cartilage with Ca^{2+} or Mg^{2+} ICR stimulation and reduced cartilage production with K^{+} tuning.

fields to alter biological properties. Zhadin [86,88] explored this question using combined AC and DC magnetic fields, to see if there might be an ICR response. The conductivity of polar amino acids in solution (Table 9.1 and Table 9.10) was chosen as an assay. The frequency of the magnetic field was swept slowly, and a single sharp current peak was observed at the cyclotronic frequency, determined from Equation 9.1 using the naked (unhydrated) molecular mass. Originally made in glutamic acid solutions [86], these observations were subsequently extended to additional amino acids, even to the case

TABLE 9.12

Opposite Responses Resulting from Shifts in Frequency or Field

Model System	Frequency (Hz)	B_0 (μT)	Ion	Response	Reference
Diatom motility	16	20.9	Ca^{2+}	Motility ↑	58
	16	41.0	K^{+}	Motility ↓	
Embryonic bone	16	20.9	Ca^{2+}	Growth ↑	24
	16	40.7	K^{+}	Growth ↓	32
Plant growth	60	78.3	Ca^{2+}	Growth ↑	75
	60	153.3	K^{+}	Growth ↓	
Rat behavior	60	48	Mg^{2+}	Learning ↑	47
	60	27	Ca^{2+}	Learning ↓	
Rat behavior	63	50	Mg^{2+}	Activity ↑	51
	38	50	Ca^{2+}	Activity ↓	
Gravitropic response	35.8	46.5	Ca^{2+}	Response ↑	79
	54.7	46.5	K^{+}	Response ↓	
Glycosaminoglycans (GAGs) concentration	16	20.9	Ca^{2+}	GAGs ↑	32
	16	40.7	K^{+}	GAGs ↓	

where it was possible to shift the ICR peak by changing the pH of the solution, and therefore the valence of the ion. This work has been independently confirmed in two-other laboratories [11,105]. One interesting aspect of these observations is the remarkably small AC magnetic field intensity required to see this effect, on the order of 0.05 μT.

It has also been shown [89] that very short (minutes) applications of ICR-tuned magnetic fields act to trigger large (days) continuing increases in conductivity in highly purified water. The required AC intensities (1 μT) are greater than that was found necessary in the Zhadin experiments, but they are still far less than reported elsewhere as interactive. The ions that are presumably affected are hydronium (H_3O^+) and its water clusters. One intriguing aspect of this work are the long-term changes in conductivity that are observed, even after removal of the magnetic field, a phenomenon somewhat akin to that of water ''memory'' [106,107].

9.3 Theoretical Approaches

9.3.1 Physical Constraints

The conditions in living things are such that charged particles are not free but subject to damping forces. If a particle such as an ion carries charge q and mass m and is moving with velocity $\mathbf{v}$, damping is manifested in the form of a retarding force, above and beyond the Lorentz force q($\mathbf{v} \times \mathbf{B}$) and the Coulomb force $q\mathbf{E}$:

$$\mathbf{F} = q(\mathbf{v} \times \mathbf{B} + \mathbf{E}) - m\mathbf{v}/\tau \tag{9.6}$$

The last term in Equation 9.6 is the mean damping force acting on the particle expressed in terms of the collision rate τ^{-1}.

The possibility of ICR occurring in living systems is counterintuitive, mainly because of damping. Cyclotron resonance, whether involving ions [108] or electrons [109], is usually associated with motion in a vacuum, or at least a low-pressure gas. In sharp contrast, the biological milieu is generally approximated as a liquid. Electron cyclotron resonance is observed in metals [109], but only at extremely high frequencies ranging from megahertz to gigahertz, many orders of magnitude greater than the typically observed frequencies listed in Table 9.3 through Table 9.10. At very high frequencies, the periodic motion of charged particles in cyclotron resonance can take place because the periods are shorter than the collision times. At 15 Hz, however, one loop is executed in 70 ms, a time over which one might expect as many as 10^{12} collisions because of thermal scattering [110]. The problem of explaining ICR effects in living systems is indeed challenging.

A second argument against the ICR hypothesis is that ions in solution are never totally free but are surrounded by layers of water. Therefore, one would think that the values of the q/m ratio indicated in Equation 9.1 would have to be lowered to reflect the extra mass that is part of the overall ionic package.

One further criticism lies in estimates of the path radius for (free) charged particles in cyclotron resonance. This is based on equating the kinetic energy $mv^2/2$ of the charged particle to the thermal energy kT, and then arguing that the radius of the particle path must necessarily reflect the resulting velocity, because this radius is given as $\rho = v(m/qB)$. At a temperature of 37°C this results in radii that are of the order of meters, much larger than the extent of the system itself. However, it is hardly clear that one can use classical kinetics to discuss low energy charged particle interactions with

molecular structures. Further, it must be noted that the cyclotronic frequency ω_c, as given in Equation 9.1 under the condition of vanishing damping, is entirely independent of particle radius and energy.

ICR tends to somewhat mute one of the strongest arguments against the likelihood of weak extremely low-frequency (ELF) magnetic interactions with biosystems. For an electric signal to initiate a biological effect, this signal must be greater than the electric potential generated by thermal noise [111]. The mean square thermal noise voltage $(\delta V)^2$ generated is proportional to Boltzmann's constant k, the temperature T, the tissue resistance R, and the bandwidth $\Delta\nu$ as follows:

$$(\delta V)^2 = 4RKT\Delta\nu \tag{9.7}$$

The original interaction site suggested by Weaver and Astumian [111] was the plasma membrane of the cell. The lipid membrane, however, is a highly electrically insulating material, with physical properties that are not conducive to any low-frequency interaction mechanism [112] except at high voltages. When more conductive substances such as proteins are considered as weak-field interaction sites, the effective resistance R can be many orders of magnitude lower than that found in lipids. Further, experimental evidence indicates that much narrower bandwidths, $\Delta\nu$, are encountered in ICR applications [39,106] than was previously [111,113] assumed. If the product $R\Delta\nu$ is reduced in Equation 9.7 by a factor of 10^{-4}, this lowers δV by a factor of 10^{-2} below the original estimates. The ''kT'' question becomes even less of a problem if one considers electric-field ICR [114], where the frequency of oscillation in Equation 9.1 is derived from endogenous sources within the living system.

9.3.2 Ion Channels

Placing the site of the ICR interaction within the lumen of membrane-bound ion channels deals with the problems of damping and hydration layers but leaves other questions unresolved. It is clear that damping within channels is quite different from that in liquids. The very function of ion channels helps define their intrinsically small effective resistivity, often less than 0.1 Ωm [115], and therefore their vanishing damping. Channels function as shunts across the insulating cell membrane, allowing ions to percolate through, often in single file [116]. The passage of ions is determined less by collision rate, as in the solution-like regions external to channels, but is more dependent on the molecular architecture [117] of the channel proteins: the gating mechanisms that permit entry into the channel lumen and the electrical potential of the atoms lining the lumen walls.

Further, this passage of ions is unencumbered by the layers of hydration that surround all ions in solution. These waters are replaced upon entry into the channel by an equivalent fixed cage lining the lumen (Figure 9.12). Although the energetics of this water replacement is still puzzling [118], there is little question that ions can pass through ion channels in a naked fashion, with no attached waters [119]. The path of ions in a channel is clearly determined in a manner that does not permit one to apply kT arguments in trivial ways.

Although one can readily deal with the two problems associated with first, damping and second, ionic hydration layers, it is not as easy to dismiss the disparity in relaxation times when one compares the very rapid passage of ions through channels to the far slower movements associated with resonance frequencies. The ratio of these times can be well in excess of 10^{10}. To illustrate the problems raised by this disparity, consider the argument that the helicity of ionic paths occurring under ICR might be such as to match the helicity of the electric potential in the lumen [120].

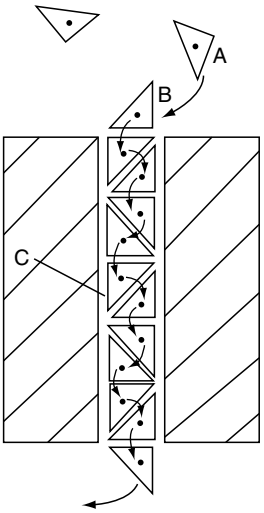

FIGURE 9.12
Hydrated ions near the mouth of an ion channel exchange their layers of water for an equivalent potential distribution within the lumen of the channel.

The electric field in Equation 9.6 can have a number of distinctly different origins. In living tissue, the electric field can be the result of endogenous sources independent of **B**. If **B** is time varying, and of sufficiently large intensity or frequency, an electric field will in addition be induced by Faraday's law. There are also experimental situations in which an electric field may be applied independently of the first two sources. When an electric field **E** is present, whatever the source, and it is at right angles to both **v** and **B**, then the circular motion becomes helical (Figure 9.13). It is then convenient to treat the velocity of the particle as composed of two components: $v_{\|}$, directed parallel to the direction of **E**, and

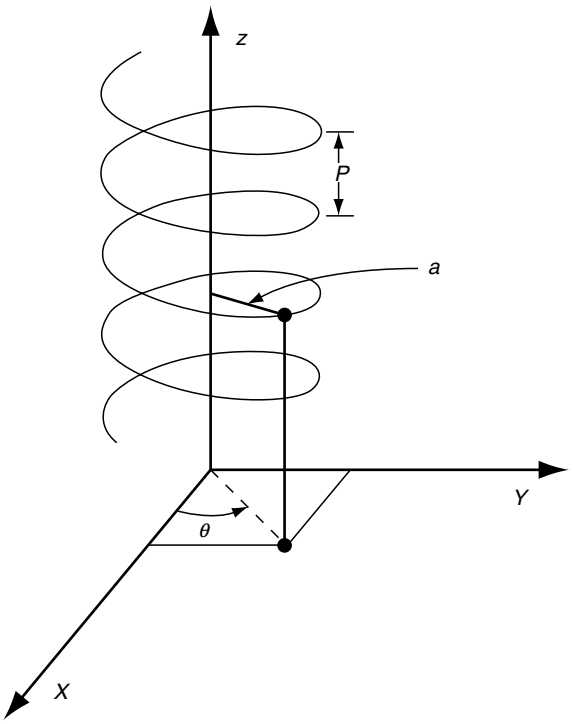

FIGURE 9.13
The Lorentz force acting on a charged particle often results in helical motion.

$v_\perp$, directed within the plane perpendicular to **E**. Then the radius of the helix is $a = mv_\perp/qB$, and its pitch is $p = 2\pi mv\|/qB$. It is not difficult to show that the total velocity v is

$$v = f_c(4\pi^2 a^2 + p^2)^{1/2} \tag{9.8}$$

The ICR frequency f_c is often only 15 Hz, and for ion channels the dimensions a and p are of the order of ångstroms (10^{-10} m). This implies a velocity of about 10^{-9} m/sec, a value that is totally inconsistent with the much greater experimentally observed speeds with which ions are transported across membranes.

Even though transit times directly through the channel lumen are very rapid, much longer relaxation times are found in other compartments of the larger channel structure. Times as long as, if not longer than, 10 ms are associated with voltage gating [121], making it conceivable that ICR could play an interactive role in channel-gating mechanisms.

9.3.3 Dependence on AC Magnetic Field

Borrowing from the theory of atomic spectroscopy [122], Lednev [7] hypothesized a functional relationship between the strength of the ICR signature and B_{AC}. When the calcium ion is bound to a calcium-binding protein such as calmodulin, the energy levels for the ion protein complex will be split, Zeeman-like, by the application of a magnetostatic field B, such that the difference in frequency between the two new levels is equal to the cyclotron resonance frequency ω_c.

Application of an AC magnetic field at this frequency then leads to a resonant condition that can alter the transition to the ground state. The ICR response itself then becomes a function of the peak value of B_{AC} expressed in terms of the probability $p(B_{AC})$ for Ca^{2+} transitions to the ground state. The field-dependent part of this probability is

$$p(B_{AC}) = (-1)^n K J_n\left(n\frac{B_{AC}}{B_0}\right) \tag{9.9}$$

where K is a constant, B_0 is the DC magnetic intensity parallel to B_{AC}, and J_n is the nth-order Bessel function having the argument nB_{AC}/B_0.

One great advantage of this expression for the probability is that one can readily design experiments that can test the predicted dependence on the AC magnetic field. Thus, the first extremum of $J_1(B_{AC}/B_0)$ occurs when the ratio B_{AC}/B_0 is equal to 1.84 (Figure 9.14). By varying this ratio while maintaining the same ICR condition, Prato et al. [72] obtained data tending to confirm this prediction. The effectiveness of this numerical ratio was also reported [74] in connection with studies on changes in calcium concentrations under ICR stimulation.

An alternative formulation to Equation 9.9 has been proposed by Blanchard and Blackman [9]. Termed ion parametric resonance (IPR) this approach considers a wider range of potential ELF interactions with metallic ions, beyond merely those processes associated with the activation of calcium-binding proteins. In the IPR formulation the probability $p(B_{AC})$ has the dependence $J_n(2nB_{AC}/B_0)$. The factor of 2 in the argument of the Bessel function has the effect of altering where the first extremum occurs, in this case at the B_{AC}/B_0 ratio of 0.92 (Figure 9.14). This ratio is close to the value of 1.0 successfully used by Smith [21,24,58,75] in all his experiments. However it is not clear in Smith's body of work whether further manipulation of the AC magnetic intensity away from this ratio of unity might have enhanced the responses that were observed. Koch et al. [91] were also able to obtain good agreement with the IPR predictions. One set of experimental results in sharp

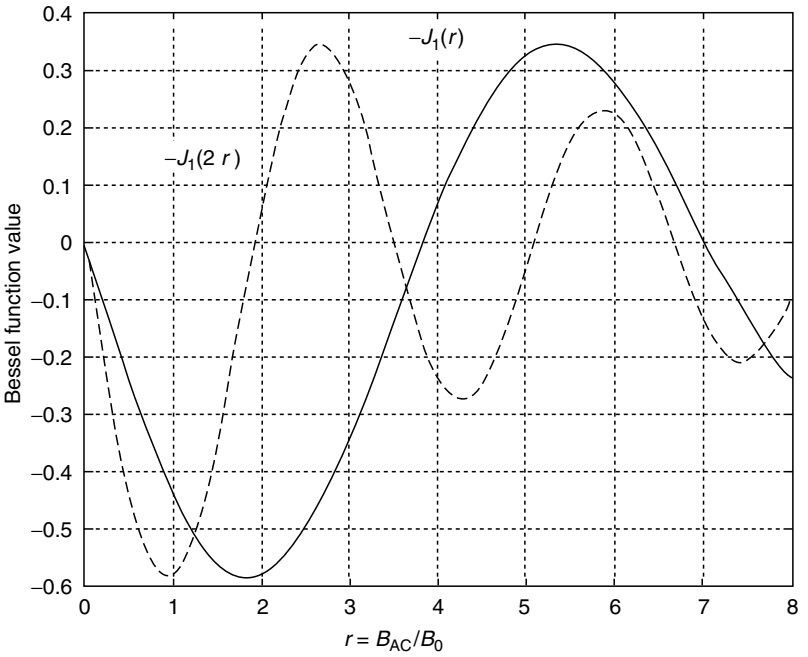

FIGURE 9.14
Comparing first-order Bessel functions with arguments B_{AC}/B_0 (solid line) and $2B_{AC}/B_0$ (dotted line). The first extremum is of experimental interest. By doubling the argument, the ratio where this extremum occurs is shifted from 1.84 to 0.92. In principle, one holds B_0 and the ICR frequency fixed and varies B_{AC} to determine where the maximum biological response occurs.

contrast with the predictions of parametric resonance are the consistent reports by Zhadin's group [86,88] and others [11], in which ICR exposures of polar amino acids in solution lead to narrow resonances, but only for B_{AC}/B_0 ratios of approximately 0.002.

The question of the dependence of the ICR interactive response on AC magnetic intensity is clouded by two additional possibilities. First, there is the problem of experimentally sorting out effects due to Faraday induction with larger AC fields [70]. Second, it is conceivable that biological responses to different AC fields may have little to do with the ICR response but rather with poorly understood physiological and energetic constraints. In any event, there is a clear record in the literature (e.g., Figure 9.15) of ICR threshold effects that do not appear to be related to functional variations such as Equation 9.9.

Adair [123,124] has criticized the parametric resonance approaches. Similar to earlier arguments [111,113] related to energetic constraints imposed by thermal noise, it was pointed out that the transition energy is only 10^{-11} of the thermal energy, kT, which would greatly suppress any meaningful effects due to Zeeman splitting. For this and other reasons [123], he concludes that application of the cyclotronic frequency ω_c cannot affect the transition rate of Ca^{2+}.

A very different approach to the problem of whether resonant magnetic fields can influence the binding of calcium has been suggested by Binhi [101]. Using Schrodinger's equation, it has been shown that ICR magnetic field combinations may redistribute the ionic probability density when one takes into account interference effects between quantum states. However, there is some question as to how much the wave function must shrink to allow ions as large as Ca^{2+} to escape.

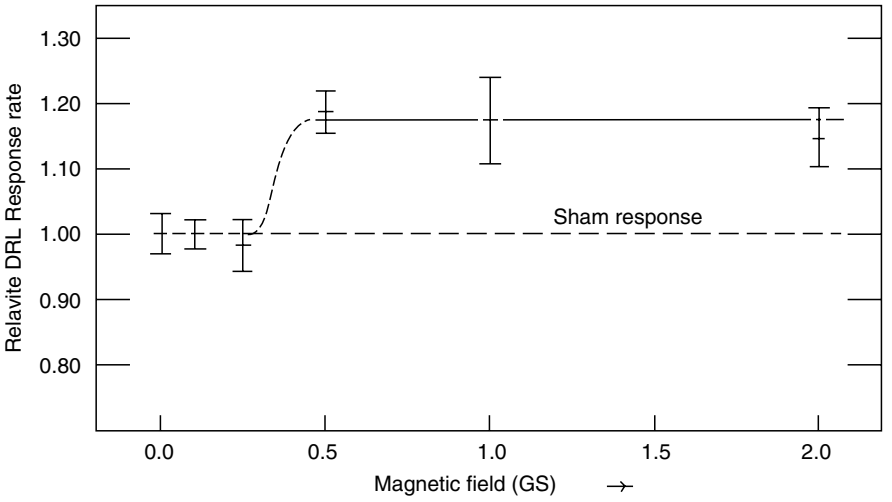

FIGURE 9.15
ICR-induced changes in rat behavior as a function of the AC magnetic field intensity. A clear threshold is evident, below which there is no effect on rat behavior. (From Liboff, A.R., Thomas, J.R., and Schrot, J., Intensity threshold for 60-Hz magnetically induced behavioral changes in rats, *Bioelectromagnetics*, 10, 111, 1989.)

9.3.4 Precessional Effects

It has been shown [8,10] that Larmor precessional effects can result from the application of weak ICR magnetic field combinations. In principle, these effects might carry physiological consequences, although no evidence along these lines has been reported. One interesting aspect of this approach [10] suggests the possibility of magnetically induced changes in the thermal energy distribution. The altered biological response in this model would not be the result of dissociative processes between ion and protein but would rather follow transfers of energy to the protein by the ion, resulting in appropriate conformational changes.

9.3.5 Coherence Domains

Del Giudice [11] has employed the principles of quantum electrodynamics (QED) in attempting to explain biological ICR, especially those results obtained in connection with the ''Zhadin Experiment'' [11,86,88]. The great advantage in this approach is that it finesses the limitations caused by Maxwell–Boltzmann statistics predictions [111,113], which require kT as a minimal threshold informational energy for electromagnetic interactions. In the QED model it is argued that in the case of electromagnetic interactions with water, coherent, highly ordered spherical domains are formed, with diameters close to 100 nm and embedded in a surrounding noncoherent water phase. An applied ICR frequency in this case couples to ions on the perimeter of the coherent spheres stimulating circulatory motion, allowing ions to escape into the noncoherent phase, where they act to enhance the measured conductivity.

One interesting aspect of this model is that because phase transitions are involved, temperature is expected to play a prominent role in the experimental outcome. The changes in amino acid conductivity under ICR conditions first reported by Novikoff and Zhadin [86] were temperature sensitive. Similar observations regarding the experimental relevance of temperature were reported in earlier [125,126] Ca-efflux studies.

9.4 Discussion

Accepting the abundant evidence that biological systems are sensitive to ICR-tuned field combinations, the question remains as to the molecular explanation. There is also the more subtle question dealing with the implications of this effect. From the physical standpoint, the seeming inability of theorists to come to grips with this phenomenon may not mean that a new physics is called for. But there is certainly good reason to believe that something is missing in the way we categorize biological function.

The fact that a low-frequency ion resonance interaction is found in an extraordinarily wide variety of organisms argues against the commonly held notion that this phenomenon merely represents one fortuitous example of the Lorentz force acting on materials that happen to occur within a biological context.

Indeed, the reports listed in Table 9.10 lend strength to another notion, that the weak-field ICR phenomenon is not limited to biological systems, but is actually a subtle physical effect that has not heretofore been recognized. For example, one can argue that this effect is particularly evident in water, which in turn results in the biological effects that are observed. In other words, because of the ubiquity of water in biological systems, any ELF-induced change in the properties of water might help explain the variety of biological effects that have been reported.

Whatever its molecular origin, it is likely that the ICR-related biophenomenon is an evolutionarily well-conserved property of the physiological armory, one that is enabled by the interaction of the ubiquitous Earth's magnetic field with the equally ubiquitous electric fields that are found throughout living things. This concept is embodied in the reasonable likelihood [114] that electric-field ICR processes were incorporated into living things over evolutionary times. Unlike the laboratory experiments involving the applications of parallel combined AC and DC magnetic fields, *E*-field resonance occurs maximally for time-varying electric and magnetostatic fields at right angles. This naturally occurring interaction therefore relates the GMF and the AC electric fields found within the biosystem. It has been hypothesized [127], for example, that this putative interaction mechanism can be used to explain the problem of bird navigation.

One can speculate that this ICR phenomenon conserved very early in living things has evolved into a number of separate biological expressions, where the physics is always the same but the physiological pathway leads to different end points. For example, two sharply different possible end points, both apparently relying on ICR, are the magnetic compasses in animals [124] and growth and repair mechanisms [24,37,75]. A third intriguing possibility is found in the ICR interactive changes in the central nervous system [45,47,49,51], an area where there are obvious effects but where the end points are still unresolved.

It is also tempting to speculate on the larger implications of the work that is detailed in Table 9.3 and Table 9.9, on bone and plants, respectively. In both cases there is evidence that ICR signals affect growth and repair responses more than they affect stasis. Drawing on possible endogenous mechanisms related to *E*-field ICR, it is conceivable that the interactive relation of the GMF to living systems is especially important as regards growth and repair during development.

Whatever be the explanation for the ICR effect, it is clear that while nothing new may be required in our understanding of physical law, new approaches are necessary in comprehending how physics has been incorporated in biology, particularly with regard to cell signaling and regulation. This is strongly implied by the remarkable data indicating reversed physiological outcomes with minor changes in electromagnetic field conditions. There are protein systems in physiology that are switch-like in their function. Two such

examples are the calcium-binding proteins and NMDA. Another example is found in synaptic transmission. The electromagnetic reversal effects observed in ICR experiments are evocative of the way such switch-like proteins function.

This begs the fascinating question as to whether the ICR stimulus merely serves as an adjunct to an existing biochemical process, perhaps acting to sharpen enhancement or inhibition, or whether it acts in a totally different manner, as a separate and distinct class of interactions, one that is completely electromagnetic in its operation. In this regard, note that the GMF preceded by far the first appearance of living things on Earth and would therefore have been part of the original physical template that determined the course of early evolution.

References

1. Jenrow, K.A. and Liboff, A.R., Electromagnetic techniques in neural therapy, in *Bioelectromagnetic Medicine*, Rosch, P.J. and Markov, M.S., Eds., Marcel Dekker, New York, 2004, Chapter 14.
2. Wertheimer, N. and Leeper, E., Electrical wiring configurations and childhood cancer, *Am. J. Epidemiol*., 109, 273–284, 1979.
3. Liboff, A.R., The charge-to-mass ICR signature in weak ELF bioelectromagnetic effects, in *Advances Electromagnetic Fields in Living Systems*, Vol. 4, Lin, J., Ed. Kluwer/Plenum, New York (in press).
4. Liboff, A.R., Geomagnetic cyclotron resonance in living cells, *J. Biol. Phys.*, 13, 99–102, 1985.
5. Tipler, P., *Physics*, 2nd ed., Vol. 2, Worth Publishers, New York, 1982, 729.
6. Zhadin, M.N. and Fesenko, E.E., Ionic cyclotron resonance in biomolecules, *Biomed. Sci*., 1, 245–250, 1990.
7. Lednev, V.V., Possible mechanism for the influence of weak magnetic fields on biological systems, *Bioelectromagnetics*, 12, 71–75, 1991.
8. Edmonds, D.T., Larmor precession as a mechanism for the detection of static and alternating magnetic fields, *Bioelectrochem. Bioenerg*., 30, 3–12, 1993.
9. Blanchard, J.P. and Blackman, C.F., Clarification and amplification of an ion parametric resonance model for magnetic field interactions with biological systems, *Bioelectromagnetics*, 15, 217–238, 1994.
10. Zhadin, M.N., Combined action of static and alternating magnetic fields on ion motion in a macromolecule: theoretical aspects, *Bioelectromagnetics*, 19, 279–292, 1998.
11. Del Giudice, E., Fleischmann, M., Preperata, G., and Talpo, G., On the ''unreasonable'' effects of ELF magnetic fields upon a system of ions *Bioelectromagnetics*, 23, 522–530, 2002.
12. Blackman, C.F., Benane, S.G., Rabinowitz, J.R., House, D.E., and Joines, W.T., A role for the magnetic field in the radiation-induced efflux of calcium ions from brain tissue *in vitro*, *Bioelectromagnetics*, 6, 327–337, 1985.
13. Bawin, S.M., Kazmarek, K.L., and Adey, W.R., Effects of modulated VHF fields on the central nervous system, *Ann. NY Acad. Sci*., 247, 74–81, 1975.
14. Blackman, C.F., Elder, J.A., Weil, C.M., Benane, S.G., Eichinger, D.C., and House, D.E., Induction of calcium-ion efflux from brain tissue by radiofrequency radiation and field strength, *Radio Sci*., 14, 93–98, 1979.
15. Blackman, C.F., Benane, S.G., Kinney, L.S., Joines, W.T., and House, D.E., Effects of ELF fields on calcium-ion efflux from brain tissue *in vivo*, *Rad. Res*., 92, 510–520, 1982.
16. Dutta, S.K., Subramaniam, A., Ghosh, B., and Parshad, R., Microwave radiation-induced calcium ion efflux from human neuroblastoma cells in culture, *Bioelectromagnetics*, 5, 71–78, 1984.
17. Blackman, C.F., Benane, S.G., House, D.E., and Joines, W.T., Effects of ELF (1–120 Hz) and modulated (50 Hz) RF fields on the efflux of calcium ions from brain tissue, *in vitro*, *Bioelectromagnetics*, 6, 1–11, 1985.

18. McLeod, B.R. and Liboff, A.R., Dynamic characteristics of membrane ions in multifield configurations of low-frequency electromagnetic radiation, *Bioelectromagnetics*, 7, 177–189, 1986.
19. McLeod, B.R. and Liboff, A.R.. Cyclotron resonance in cell membranes: the theory of the mechanism, in *Mechanistic Approaches to Interactions of Electric and Electromagnetic Fields with Living Systems*, Blank, M. and Findl, E., Eds., Plenum Press, New York, 1987, 97–108.
20. McLeod, B.R., Smith, S.D., and Liboff, A.R., Calcium and potassium cyclotron resonance curves and harmonics in diatoms, *J. Bioelectr.*, 6, 153–168, 1987.
21. Smith, S.D., McLeod, B.R., and Liboff, A.R., Testing the ion cyclotron resonance theory of electromagnetic field interaction with odd and even harmonic tuning for cations, *Bioelectrochem. Boenerg.*, 38, 161–167, 1995.
22. Liboff, A.R. and McLeod, B.R., Kinetics of channelized membrane ions in magnetic fields, *Bioelectromagnetics*, 9, 39–51, 1988.
23. Ross, S.M., Combined DC and ELF magnetic fields can alter cell proliferation, *Bioelectromagnetics*, 11, 27–36, 1990.
24. Smith, S.D., Liboff, A.R., and McLeod, B.R., Effects of resonant mcLeod fields on chick femoral development *in vitro, J. Bioelectr.*, 10, 81–99, 1991.
25. Fitzsimmons, R.J., Baylink, D.J., Ryaby, J.T., and Magee, F., EMF-stimulated bone-cell proliferation, in *Electricity and Magnetism in Biology and Medicine*, Blank, M., Ed., San Francisco Press, San Francisco, 1993, 899–901.
26. Ryaby, J.T., Grande, D.A., Magee, F.P., and Weinstein, A.M., The effects of combined AC/DC magnetic fields on resting articular cartilage metabolism, in *Electricity and Magnetism in Biology and Medicine*, Blank, M., Ed., San Francisco Press, San Francisco, 1993, 371–374.
27. Ryaby, J.T., Magee, F.P., Weinstein, A.M., Fitzsimmons, R.J., and Baylink, D.J., Prevention of experimental osteopenia by use of combined magnetic fields, in *Electricity and Magnetism in Biology and Medicine*, Blank, M., Ed., San Francisco Press, San Francisco, 1993, 807–810.
28. Fitzsimmons, R.J., Ryaby, J.T., Magee, F.P., and Baylink, D.J., Combined magnetic fields increased net calcium flux in bone cells. *Calcif. Tissue Int.*, 55, 376–380, 1994.
29. Diebert, M.C., McLeod, B.R., Smith, S.D., and Liboff, A.R., Ion resonance electromagnetic field stimulation of fracture healing in rabbits with a fibular ostectomy, *J. Orthop. Res.*, 12, 878–885, 1994.
30. Fitzsimmons, R.J., Ryaby, J.T., Magee, F.P., and Baylink, D.J., Combined magnetic fields increase insulin-like growth factor-II in TE-85 human osteosarcoma bone cell cultures, *Endocrinology*, 136, 3100–3106, 1995.
31. Fitzsimmons, R.J., Ryaby, J.T., Magee, F.P., and Baylink, D.J., IGF-II receptor number is increased in TE-85 human osteosarcoma cells by combined magnetic fields, *J. Bone Miner. Res.*, 10, 812–819, 1995.
32. Regling, C., Brueckner, C., Liboff, A.R., and Kimura, J.H., Evidence for ICR magnetic field effects on cartilage and bone development in embryonic chick bone explants (abstract), 48th Annual Meeting, Orthopedic Research Society, Dallas, 2002.
33. Liboff, A.R., Rozek, R.J., Sherman, M.L., McLeod, B.R., and Smith, S.D., $_{45}Ca^{2+}$ resonance in human lymphocytes. *J. Bioelectr.*, 6, 99–102, 1987.
34. Rozek, R.J., Sherman, M.L., Liboff, A.R., McLeod, B.R., and Smith, S.D., Nifedipene is an antagonist to cyclotron resonance enhancement of 45Ca incorporation in human lymphocytes, *Cell Calcium*, 8, 413–427, 1987.
35. Parkinson, W.C. and Hanks, C.T., Search for cyclotron resonance in cells *in vitro*, *Bioelectromagnetics*, 10, 129–145, 1989.
36. Rochev, Y.A., Narimanov, A.A., Sosunov, E.A., Kozlov, A.N., and Lednev, V.V., Effects of weak magnetic field on the rate of cell proliferation in cell culture, *Stud. Biophys.*, 135, 93–98, 1990.
37. Lyle, D.B., Wang, X., Ayotte, R.D., Sheppard, A.R., and Adey, W.R., Calcium uptake by leukemic and normal T-lymphocytes exposed to low frequency magnetic fields, *Bioelectromagnetics*, 12, 145–156, 1991.
38. Yost, M.G. and Liburdy, R.P., Time-varying and static magnetic fields act in combination to alter calcium signal transduction in the lymphocyte, *FEBS Lett.*, 296, 117–122, 1992.
39. Liboff, A.R., Jenrow, K.A., and McLeod, B.R., ELF-induced proliferation at 511 mG in HSB-2 cell culture as a function of 60 Hz field intensity, in *Electricity and Magnetism in Biology and Medicine*, Blank, M., Ed., San Francisco Press, San Francisco, 1993.

40. Liburdy, R.P. and Yost, M.G., Time-varying and static magnetic fields act in combination to alter calcium signal transduction in the lymphocyte, in *Electricity and Magnetism in Biology and Medicine*, Blank, M., Ed., San Francisco Press, San Francisco, 1993.
41. Coulton, L.A. and Barker, A.T., Magnetic fields and intracellular calcium: effects on lymphocytes exposed to conditions for ''cyclotron resonance'', *Phys. Med. Biol*., 38, 347–360, 1993.
42. Lindstrom, E., Lindstrom, P., Berglund, A., Lundgren, E., and Mild, K.H., Intracellular calcium oscillations in a T-cell line after exposure to extremely-low-frequency magnetic fields with variable frequencies and flux densities, *Bioelectromagnetics*, 16, 41–47, 1995.
43. Tofani, S., Ferrara, A., Anglesio, L., and Gilli, G., Evidence for genotoxic effects of resonant ELF magnetic fields, *Bioelectrochem. Bioenerg*., 36, 9–13, 1995.
44. Reinbold, K.A. and Pollack, S.R., Serum plays a critical role in modulating $[Ca^{2+}]_c$ of primary cell culture bone cells exposed to weak ion-resonance magnetic fields, *Bioelectromagnetics*, 18, 203–214, 1997.
45. Thomas, J.R., Schrot, J., and Liboff, A.R., Low-intensity magnetic fields alter operant behavior in rats, *Bioelectromagnetics*, 7, 349–357, 1986.
46. Liboff, A.R., Thomas, J.R., and Schrot, J., Intensity threshold for 60-Hz magnetically induced behavioral changes in rats, *Bioelectromagnetics*, 10, 111–113, 1989.
47. Lovely, R.H., Creim, J.A., Miller, D.L., and Anderson, L.E., Behavior of rats in a radial arm maze during exposure to magnetic fields: evidence for effects of magnesium ion resonance (abstract), 15th Annual Meeting, Bioelectromagnetics Society, Los Angeles, 1993.
48. Stern, S., Laties, V.G., Nguyen, Q.A., and Cox, C., Exposure to combined static and 60Hz magnetic fields: failure to replicate a reported behavioral effect, *Bioelectromagnetics*, 17, 279–292, 1996.
49. Lyskov, Y.B., Chernysev, M.V., Michailov, V.O., Kozlov, A.P., Makarova, T.M., Vasilyeva, Y.V., Druzin, M.Y., Sokolov, G.V., and Vishnevski, A.M., The effect of a magnetic field with the frequency of 50 Hz on behavior in rats depends on the value of the constant magnetic field, *Biophysics*, 41, 881–886, 1996.
50. Derjugina, O.N., Pisachenko, T.M., and Zhadin, M.N., Combined action of alternating and static magnetic fields on behavior of rats in the ''Open-field'' test, *Biophysics*, 41, 762–764, 1996.
51. Zhadin, M.N., Deryugina, O.N., and Pisachenko, T.M., Influence of combined DC and AC magnetic fields on rat behavior, *Bioelectromagnetics*, 20, 378–386, 1999.
52. Smith, S.D., Liboff, A.R., McLeod, B.R., and Barr, E.J., Effects of ion resonance tuned magnetic fields on N-18 neuroblastoma cells, in *Charge and Field Effects in Biosystems-3*, Allen, M.J., Cleary, A.F., Sowers, A.E., and Shillady, D.D., Eds., Birkhauser, Boston, 1992, 263–271.
53. Horton, P., Ryaby, J.T., Magee, F.P., and Weinstein, A.M., Stimulation of specific neuronal differentiation proteins in PC-12 cells by combined AC/DC magnetic fields, in *Electricity and Magnetism in Biology and Medicine*, Blank, M., Ed., San Francisco Press, San Francisco, 1993, 619–622.
54. Blackman, C.F., Blanchard, J.P., Benane, S.G., and House, D.E., Empirical test of an ion parametric resonance model for magnetic field interactions with PC-12 cells, *Bioelectromagnetics*, 15, 239–250, 1994.
55. Trillo, M.A., Ubeda, A., Blanchard, J.P., House, D.E., and Blackman, C.F., Magnetic fields at resonant conditions for the hydrogen atom can affect neurite outgrowth in PC-12 cells, *Bioelectromagnetics*, 17, 10–20, 1996.
56. Blanchard, J.P., Blackman, C.F, Benane, S.G., and House, D.E., IPR response of PC-12 cells exposed to magnetic fields tuned for calcium ions, The Annual Review of Research on Biological Effects of Electric and Magnetic Fields from the Generation, Delivery and Use of Electricity, San Diego, CA, W/L Associates, Ltd, Frederick, MD, 1997, 4.
57. Blackman, C.F., Blanchard, J.P., Benane, S.G., and House, D.E., Experimental determination of hydrogen bandwidth for the Ion Parametric Resonance model, *Bioelectromagnetics*, 20, 5–12, 1999.
58. Smith, S.D., McLeod, B.R., Liboff, A.R., and Cooksey, K., Calcium cyclotron resonance and diatom motility, *Bioelectromagnetics*, 8, 215–227, 1987.
59. McLeod, B.R., Smith, S.D., Cooksey, K.E., and Liboff, A.R., Ion cyclotron resonance frequencies enhance Ca^{2+}-dependent motility in diatoms, *J. Bioelectr*., 6, 1–12, 1987.
60. McLeod, B.R., Smith, S.D., and Liboff, A.R., Calcium and potassium cyclotron resonance curves and harmonics in diatoms, *J. Bioelectr*., 6, 153–168, 1987.

61. Reese, J.A, Frazier, M.E., Morris, J.E., Buschbom, R.L., and Miller, D.L., Evaluation of changes in diatom motility after exposure to 16-Hz electromagnetic fields, *Bioelectromagnetics*, 12, 21–25, 1991.
62. Parkinson, W.C. and Sulik, G.L., Diatom response to extremely low frequency magnetic fields, *Rad. Res*., 130, 319–330, 1992.
63. Saalman, E., Galt, S., Hamnerius, Y., and Norden, B., Diatom motility: replication study in search of cyclotron resonance effects, in *Interaction Mechanisms of Low-Level Electromagnetic Fields in Living Systems*, Norden, B. and Ramel, C., Eds., Oxford University Press, Oxford, 1992, 280–292.
64. Prasad, A.V., Miller, M.W., Cox, C., Carstensen, E.L., Hops, H., and Brayman, A.A., A test of the influence of cyclotron resonance exposures on diatom motility, *Health Phys*., 66, 305–312, 1994.
65. Clarkson, H., Davies, M.S., and Dixey, R., Diatom motility: the search for independent replication of biological effects of extremely low-frequency electromagnetic fields, *Int. J. Rad. Biol*., 75, 387–392, 1999.
66. Liboff, A.R. and Parkinson, W.C., Search for ion-cyclotron resonance in an Na^+ transport system, *Bioelectromagnetics*, 12, 77–83, 1991.
67. Lerchl, A., Reiter, R.J., Nonaka, K.O., and Stokken, K.-A., Evidence that extremely low frequency Ca^{2+}-cyclotron resonance depresses pineal melatonin synthesis *in vitro*, *Neurosci. Lett*., 124, 213–215, 1991.
68. Chemeris, N.K. and Safranova, V.G., Weak low-frequency magnetic field initiates frequency-dependent fluctuations of period of Daphnia magna's heart beatings, *Biophysics*, 38, 511–519, 1993.
69. Jenrow, K.A., Smith, C.H., and Liboff, A.R., Weak extremely-low-frequency magnetic fields and regeneration in the planarian Dugesia tigrina, *Bioelectromagnetics*, 16, 106–112, 1995.
70. Jenrow, K.A., Smith, C.H., and Liboff, A.R., Weak, extremely-low-frequency magnetic field-induced regeneration anomalies in the planarian Dugesia tigrina, *Bioelectromagnetics*, 17, 467–474, 1996.
71. Tiras, K.P., Srebnitskaya, L.K., Il'jasova, A.A., and Lednev, V.V., The influence of weak combined magnetic fields on the rate of regeneration in planarian Dugesia tigrina, *Biophysics*, 42, 826–831, 1996.
72. Prato, F.S., Kavaliers, M., Cullen, A.P., and Thomas, A.W., Light-dependent and -independent behavioral effects of extremely low frequency magnetic fields, *Bioelectromagnetics*, 18, 284–291, 1997.
73. Prato, F.S., Kavaliers, M., and Thomas, A.W., Extremely low frequency magnetic fields can either increase or decrease analgesia in the land snail depending on field and light conditions, *Bioelectromagnetics*, 21, 287–301, 2000.
74. Berden, M., Zrimec, A., and Jerman, I., New biological detection system for weak ELF magnetic fields and testing of the parametric resonance model, *Electro. Magnetobiol*., 20, 27–41, 2001.
75. Smith, S.D., McLeod, B.R., and Liboff, A.R., Effects of CR-tuned 60 Hz magnetic fields on sprouting and early development of *Raphanus sativus*, *Bioelectr. Bioenerg*., 32, 67–76, 1993.
76. Davies, M.S., Effects of 60 Hz electromagnetic fields on early growth in three plant species and a replication of previous results, *Bioelectromagnetics*, 17, 154–161, 1996.
77. Tohtz, S.W., The Influence of Ultra Weak Magnetic Fields on Growth and Differentiation Using the ICR Hypothesis: An Experimental Study on Radish Seedlings and a Theoretical Discussion on Relevant Aspects of Cartilage, Bone, and Other Connective Tissues, Ph.D. Dissertation, Medical Faculty of Humboldt University, Berlin, 1996 (in German).
78. Smith, S.D., Liboff, A.R., and McLeod, B.R., Potassium ion cyclotron resonance magnetic fields stimulate germination, Proceedings of Millennium International Workshop on Biological Effects of Electromagnetic Fields, Heraclion, Crete, Greece, 2000, 347–351.
79. Belova, N.A. and Lednev, V.V., Activation and inhibition of gravitropic response in plants by weak combined magnetic fields, *Biophysics*, 45, 1069–1074, 2000.
80. Belova, N.A. and Lednev, V.V., Dependence of gravitropic response in the segments of flax stems on the frequency and amplitude of weak combined magnetic fields, *Biophysics*, 45, 1075–1078, 2000.
81. Yano, A., Ohashi, Y., Hirasaki, T., and Fujiwara, K., Effects of a 60 Hz magnetic field on photosynthetic CO_2 uptake and early growth of radish seedlings, *Bioelectromagnetics*, 25, 572–581, 2004.

82. Shuvalova, L.A., Ostrovskaja, M.V., Sosunov, E.A., and Lednev, V.V., Effect of weak magnetic field in the parametric resonance mode on the rate of calmodulin-dependent phosphorylation of myosin in the solution, Doklady Akademii Nauk SSSR (Reports of the Academy of Science of the USSR), Vol. 317, 1991, 227–230 (in Russian).
83. Durney, C.H., Kaminski, M., Anderson, A.A., Bruckner-Lea, C., and Rappaport, C., Investigation of AC–DC magnetic field effects in planar phospholipid layers, *Bioelectromagnetics*, 13, 19–33, 1992.
84. Bruckner-Lea, C., Durney, C.H., Janata, J., Rappaport, C., and Kaminski, M., Calcium binding to metallochromic dyes and calmodulin in the presence of combined AC–DC magnetic fields, *Bioelectromagnetics*, 13, 147–162, 1992.
85. Galt, S., Sandblom, A., Hamnerius, Y., Hojevic, P., Saalman, E., and Norden, B., Experimental search for combined AC and DC magnetic field effects on ion channels, *Bioelectromagnetics*, 14, 315–327, 1993.
86. Novikoff, V.V. and Zhadin, M.N., Combined action of weak constant and variable low-frequency magnetic fields on ionic currents in aqueous solutions of amino acids, *Biophysics*, 39, 41–45, 1994.
87. Hojevic, P., Sandblom, J., Galt, S., and Hamnerius, Y., Ca^{2+} ion transport through patch-clamped cells exposed to magnetic fields, *Bioelectromagnetics*, 16, 33–40, 1995.
88. Zhadin, M.N., Novikoff, V.V., Barnes, F.S., and Pergola, M.F., Combined action of static and alternating magnetic fields on ionic current in aqueous glutamic acid solution, *Bioelectromagnetic*s, 19, 41–45, 1998.
89. Mohri, K., and Fukushima, M., Gradual decreasing characteristics and temperature stability of electric resistivity in water triggered with milligauss AC field, *IEEE Trans. Magn.*, 38, 3353–3355, 2002.
90. Liboff, A.R., Cherng, S., Jenrow, K.A., and Bull, A., Calmodulin dependent cyclic nucleotide phosphodiesterase activity is altered by 20 μT magnetostatic fields, *Bioelectromagnetics*, 24, 32–38, 2002.
91. Koch, C.L.M.B., Sommarin, M., Perrson, B.R.R., Salford, L.G., and Eberhardt, J.L., Interaction between weak low frequency magnetic fields and cell membranes, *Bioelectromagnetics*, 24, 395–402, 2003.
92. Creim, J.A., Lovely, R.H., Miller, D.L., and Anderson, L.E., Rats can discriminate illuminance, but not magnetic fields, as a stimulus for learning a two-choice discrimination, *Bioelectromagnetics*, 23, 545–549, 2002.
93. Tang, Y-P., Shimizu, E., Dube, G.R., Rampon, C., Kerchner, G.A., Zhuo, M., Liu, G., and Tsien, J.Z., Genetic enhancement of learning and memory in mice, *Nature*, 401, 63–69, 1999.
94. Muller, D., and Lynch, G., Synaptic modulation of *N*-methyl D-aspartate receptor mediated responses in hippocampus, *Synapse*, 5, 94–103, 1990.
95. Shiekhattar, R. and Aston-Jones, G., NMDA-receptor-mediated sensory responses of brain noradrenergic neurons are suppressed by *in-vivo* concentrations of extracellular magnesium, *Synapse*, 10, 103–109, 1992.
96. Smith, S.D., Liboff, A.R., and McLeod, B.R., Calcium ICR and seedling growth in orchids (abstract), 20th Annual Meeting, Bioelectromagnetics Society, St. Petersburg Beach, FL, 1998.
97. Poggi, C., private communication, 2004.
98. Bassett, C.A.L., Pawluk, R.J., and Pilla, A.A., Acceleration of fracture repair by electromagnetic fields: a surgically non-invasive method, in *Electrically Mediated Growth Mechanisms in Living Systems*, Liboff, A.R. and Rinaldi, R.A., Eds., *Ann. NY Acad. Sci.*, 238, 242–262, 1974.
99. Liboff, A.R., Electrical treatment of ununited bone fracture and spinal fusion, in *Encyclopedia of Medical Devices*, 2nd ed., Webster, Ed., John Wiley, New York, 2005.
100. Blackman, C.F., Benane, S.G., Elliott, D.J., House, D.E., and Pollock, M.M., Influence of electromagnetic fields on the efflux of calcium ions from brain tissue *in vitro*: a three-model analysis consistent with the frequency response up to 510 Hz, *Bioelectromagnetics*, 9, 215–227, 1988.
101. Binhi, V.N., Amplitude and frequency dissociation spectra of ion-protein complexes rotating in magnetic fields, *Bioelectromagnetics*, 21, 34–45, 2000.
102. Liboff, A.R., Comment on ''Extremely low frequency magnetic fields can either increase or decrease analgesia in the Land Snail depending on field and light conditions'', *Bioelectromagnetics*, 23, 406–407, 2002.

103. Ayrapetyan, S., Grigorian, K., Avanesyan, A., and Stamboltsian, K., Magnetic fields alter electrical properties of solutions and their physiological effects, *Bioelectromagnetics*, 15, 133–142, 1994.
104. Rai, S., Singh, U., Singh, K., and Singh, A., Germination responses of fungal spores to magnetically restructured water, *Electro. Magnetobiol*., 13, 237–246, 1994.
105. Ruzic, R. and Jerman, I., Influence of Ca^{2+} in biological effects of direct and indirect ELF magnetic field stimulation, *Electro. Magnetobiol*., 17, 205–216, 1998.
106. Pazur, A., Characterization of weak magnetic field effects in an aqueous glutamic acid solution by nonlinear dielectric spectroscopy and voltammetry, *Biomagn. Res. Technol*., 2, 1–18, 2004.
107. Binhi, V.N., *Magnetobiology*, Academic Press, London, 2002, 333–343.
108. Beauchamp, J.L., Ion cyclotron resonance spectroscopy, *Ann. Rev. Phys. Chem*., 22, 527–561, 1971.
109. Azbel, M.Ya. and Kaner, E.A., Cyclotron resonance in metals, *J. Phys. Chem. Solids*, 6, 113–135, 1958.
110. Hobbie, R.K., *Intermediate Physics for Medicine and Biology*, 3rd ed., Springer, New York, 1997, 83–84.
111. Weaver, J.C. and Astumian, R.D., The response of living cells to very weak magnetic fields: the thermal noise limit, *Science*, 247, 459–462, 1990.
112. Liboff, A.R. and Jenrow, K.A., Cell sensitivity to magnetic fields, *Electro. Magnetobiol*., 19, 223–236, 2000.
113. Adair, R.K., Constraints on biological effects of weak extremely-low-frequency electromagnetic fields, *Phys. Rev. A*, 43, 1039–1048, 1991.
114. Liboff, A.R., Electric-field ion cyclotron resonance, *Bioelectromagnetics*, 18, 85–87, 1997.
115. Aidley, D.J. and Stanfield, P.B., *Ion Channels*, Cambridge University Press, Cambridge, 1996, 146.
116. Nelson, P.H., A permeation theory for single-file ion channels: concerted-association/dissociation, *J. Chem. Phys*., 119, 6981–6982, 2003.
117. Yellen, G., Permeation in potassium channels: implications for channel structure, *Ann. Rev. Biophys. Biophys. Chem*., 16, 227–246, 1987.
118. Liboff, A.R., Ion cyclotron resonance in biological systems: experimental evidence, in *Biological Effect of Electromagnetic Fields*, Stavroulakis, P., Ed., Springer, Berlin, 2003, 76–113.
119. Hille, B., *Ionic Channels of Excitable Membranes*, Sinauer Associates, Sunderland, MA, 183, 1984.
120. Li-Smerin, Y., Hackos, D.H., and Swartz, K.J., α-Helical structural elements within the voltage-sensing domain of a K^+ channel, *J. Gen. Physiol*., 115, 33–49, 2000.
121. Kuyucak, S., Andersen, O.S., and Chung, S.-H., Models of permeation in ion channels, *Rep. Prog. Phys*., 64, 1427–1472, 2001.
122. Lednev, V., Interference with the vibrational energy sublevels of ions bound in calcium-binding proteins as the basis for the interaction of weak magnetic fields with biological systems, in *On the Nature of Weak Magnetic Fields with Biological Systems*, Frey, A.H., Ed., Landes, Austin, TX, 1994, Chapter 5.
123. Adair, R.K., Criticism of Lednev's mechanism for the influence of weak magnetic field on biological systems, *Bioelectromagnetics*, 13, 231–235, 1992.
124. Adair, R.K., A physical analysis of the ion parametric resonance mode, *Bioelectromagnetics*, 19, 181–191, 1998.
125. Lee, Q.P., Guy, A.W., Lai, H., and Horita, A., The effects of modulated radiofrequency radiation on calcium efflux from chick brains *in vitro* (abstract), 9th Annual Meeting, Bioelectromagnetics Society, Portland, OR, 1987.
126. Blackman, C.F., Benane, S.G., and House, D.G., The influence of temperature during electric- and magnetic-field induced alteration of calcium-ion release from *in vitro* brain tissue, *Bioelectromagnetics*, 12, 173–182, 1991.
127. Liboff, A.R. and Jenrow, K.A., New model for the avian magnetic compass, *Bioelectromagnetics*, 21, 555–565, 2000.